# CD1d-restricted peripheral T cell lymphoma in mice and humans

Emmanuel Bachy,[1,2,3,4,5,6,11] Mirjam Urb,[1,2,3,4,5] Shilpi Chandra,[12] Rémy Robinot,[1,2,3,4,5] Gabriel Bricard,[1,2,3,4,5] Simon de Bernard,[13] Alexandra Traverse-Glehen,[7,14] Sophie Gazzo,[8,14] Olivier Blond,[15] Archana Khurana,[12] Lucile Baseggio,[9,14] Tayla Heavican,[16] Martine Ffrench,[9,14] Giuliano Crispatzu,[17] Paul Mondière,[1,2,3,4,5] Alexandra Schrader,[17] Morgan Taillardet,[1,2,3,4,5] Olivier Thaunat,[1,2,3,4,5] Nadine Martin,[18,19,20] Stéphane Dalle,[10,21,22] Magali Le Garff-Tavernier,[23,24] Gilles Salles,[6,11,14] Joel Lachuer,[11,22,25] Olivier Hermine,[26,27] Vahid Asnafi,[28] Mikael Roussel,[29] Thierry Lamy,[29] Marco Herling,[17] Javeed Iqbal,[16] Laurent Buffat,[13] Patrice N. Marche,[15] Philippe Gaulard,[18,19,20] Mitchell Kronenberg,[12] Thierry Defrance,[1,2,3,4,5] and Laurent Genestier[1,2,3,4,5]

[1]CIRI, International Center for Infectiology Research, Université de Lyon, 69007 Lyon, France
[2]Institut National de la Santé et de la Recherche Médicale (INSERM), U1111, 69007 Lyon, France
[3]Ecole Normale Supérieure de Lyon, 69007 Lyon, France
[4]Université Lyon 1, Centre International de Recherche en Infectiologie, 69007 Lyon, France
[5]Centre National de la Recherche Scientifique (CNRS), UMR 5308, 69365 Lyon, France
[6]Department of Hematology, [7]Department of Pathology, [8]Department of Cytogenetics, [9]Department of Cytology, and [10]Department of Dermatology, Centre Hospitalier Lyon-Sud, Hospices Civils de Lyon, 69004 Lyon, France
[11]Université de Lyon, Université Claude Bernard Lyon1, 69007 Lyon, France
[12]Division of Developmental Immunology, La Jolla Institute for Allergy and Immunology, La Jolla, CA 92037
[13]AltraBio SAS, 69007 Lyon, France
[14]CNRS, UMR 5239, 69342 Lyon, France
[15]Institut Albert Bonniot, INSERM U823, Université J. Fourier, 38041 Grenoble, France
[16]Department of Pathology and Microbiology, Center for Lymphoma and Leukemia Research, University of Nebraska Medical Center, Omaha, NE 68198
[17]Laboratory of Lymphocyte Signaling and Oncoproteome, Department I of Internal Medicine, Center for Integrated Oncology Köln-Bonn, and Excellence Cluster for Cellular Stress Response and Aging-Associated Diseases, University of Cologne, 50923 Cologne, Germany
[18]INSERM U955 and [19]Université Paris-Est, Créteil 94000, France
[20]Department of Pathology, AP-HP, Groupe Henri-Mondor Albert-Chenevier, 94000 Créteil, France
[21]University Claude Bernard Lyon 1, 69100 Lyon, France
[22]INSERM UMR-S1052, CNRS UMR 5286, Centre de Recherche en Cancérologie de Lyon, 69003 Lyon, France
[23]Service d'Hématologie Biologique, Groupe Hospitalier Pitié-Salpêtrière, Sorbonne Universités, UPMC, Université Paris 06 et Assistance Publique-Hôpitaux de Paris, 75004 Paris, France
[24]INSERM U1138, Programmed cell death and physiopathology of tumor cells, Centre de Recherche des Cordeliers, 75006 Paris, France
[25]ProfileXpert, SFR Santé Lyon-Est, UCBL UMS 3453 CNRS-US7 INSERM, 69372 Lyon, France
[26]Institut Imagine, Laboratoire INSERM, Unité Mixte de Recherche 1163, CNRS Équipe de Recherche Laboratoryéllisée 8254, Cellular and Molecular Basis of Hematological Disorders and Therapeutic Implications, 75015 Paris, France
[27]Service d'Hématologie, Faculté de Médecine Paris Descartes, Sorbonne Paris-Cité et Assistance Publique-Hôpitaux de Paris Hôpital Necker, 75015 Paris, France
[28]Université Paris Descartes Sorbonne Cité, Institut Necker-Enfants Malades, INSERM U1151, and Laboratory of Onco-Hematology, Assistance Publique-Hôpitaux de Paris, Hôpital Necker Enfants-Malades, 75015 Paris, France
[29]Rennes University Hospital, Rennes INSERM UMR 917 Faculté de Médecine Université Rennes 1, 35000 Rennes, France

**Peripheral T cell lymphomas (PTCLs) are a heterogeneous entity of neoplasms with poor prognosis, lack of effective therapies, and a largely unknown pathophysiology. Identifying the mechanism of lymphomagenesis and cell-of-origin from which PTCLs arise is crucial for the development of efficient treatment strategies. In addition to the well-described thymic lymphomas, we found that p53-deficient mice also developed mature PTCLs that did not originate from conventional T cells but from CD1d-restricted NKT cells. PTCLs showed phenotypic features of activated NKT cells, such as PD-1 up-regulation and loss of NK1.1 expression. Injections of heat-killed *Streptococcus pneumonia*, known to express glycolipid antigens activating NKT cells, increased the incidence of these PTCLs, whereas *Escherichia coli* injection did not. Gene expression profile analyses indicated a significant down-regulation of genes in the TCR signaling pathway in PTCL, a common feature of chronically activated T cells. Targeting TCR signaling pathway in lymphoma cells, either with cyclosporine A or anti-CD1d blocking antibody, prolonged mice survival. Importantly, we identified human CD1d-restricted lymphoma cells within Vδ1 TCR-expressing PTCL. These results define a new subtype of PTCL and pave the way for the development of blocking anti-CD1d antibody for therapeutic purposes in humans.**

Correspondence to Laurent Genestier: laurent.genestier@inserm.fr

M. Urb, R. Robinot, and L. Genestier's present address is Centre de Recherche en Cancérologie de Lyon, INSERM U1052, Faculté de Médecine Lyon-Sud 165, 69921 Oullins, France.



The Rockefeller University Press $30.00
J. Exp. Med. 2016 Vol. 213 No. 5 841–857
www.jem.org/cgi/doi/10.1084/jem.20150794

Non-Hodgkin lymphoma is a form of cancer that emerges from the transformation of mature B, T, or NK cells. Peripheral T cell lymphomas (PTCLs) represent 12–15% of all lymphoid malignancies in Western countries and include >20 entities that can be grouped according to their presentation as disseminated (leukemic), predominantly extranodal, cutaneous, or predominantly nodal diseases (Swerdlow et al., 2008). Chemotherapy regimens that cure many patients with B cell lymphomas have produced disappointing results in PTCL so far, explaining a dismal prognosis with a 5-yr overall survival rate barely exceeding 30%. Furthermore, compared with the breakthrough achieved by anti-CD20 and BCR pathway inhibitors currently revolutionizing the management of B cell malignancies, no major advances have been made during the last decades in the study of PTCLs, emphasizing the need for innovative approaches.

Identifying the cell origin from which lymphomas arise is a field of intense research and has been fruitfully applied to B cell lymphoma classification (Swerdlow et al., 2008). Unraveling the correlations between B cell lymphoma subtypes and normal B cell development has helped to understand transformation mechanisms, formed the basis for the current classification of B cell lymphomas in humans, and, most importantly, contributed to tailored therapeutic strategies. Such a link between normal T cell developmental stages and the cellular origin in T cell lymphomas is poorly elucidated. Except for angioimmunoblastic T cell lymphoma, whose normal counterpart was identified as follicular helper T cells, the cell-of-origin for most mature T cell malignancy is still a matter of speculation (de Leval et al., 2007). The complexity of the T cell branch of adaptive immunity, encompassing numerous subsets of conventional (restricted by MHC molecules) and unconventional (restricted by MHC-like molecules) T cells (Salio et al., 2014) with effector, memory, and regulatory functions, might explain why PTCLs are still poorly defined.

Among unconventional T cells, invariant natural killer T cells (iNKT cells) represent a peculiar subset exhibiting several unusual properties. First, they express an invariant TCR α chain composed of a rearrangement of Vα14-Jα18, with a conserved CDR3α region generated by the rearrangement (Bendelac et al., 2007). Second, whereas conventional T cells recognize peptide fragments, iNKT cells recognize self-antigens and microbial lipid-containing antigens presented by CD1d, a nonpolymorphic MHC class I–like antigen-presenting molecule (Bendelac et al., 2007). Third, iNKT cells very rapidly produce several effector cytokines and, like innate immune cells, they lack a clear memory response.

Abbreviations used: ALK, anaplastic lymphoma kinase; αGalCer, α-galactosylceramide; CsA, cyclosporine A; GEP, gene expression profile; GO, gene ontology; GSEA, gene set enrichment analysis; HEtE, hematoxylin and eosin; HSTL, hepatosplenic T cell lymphoma; iNKT, invariant NKT; MAIT, mucosal invariant T; MFI, mean fluorescence intensity; M-FISH, multicolor fluorescence in situ hybridization; PCA, principal component analysis; PLZF, promyelocytic leukemia zinc finger; PTCL, peripheral T cell lymphoma; PTCL-NOS, PCTL-not otherwise specified; Spn, *Streptococcus pneumonia*; TdT, terminal deoxynucleotidyl transferase; TL, thymic lymphoma; T-LGL, T cell large granular lymphocyte leukemia; T-PLL, T cell prolymphocytic leukemia.

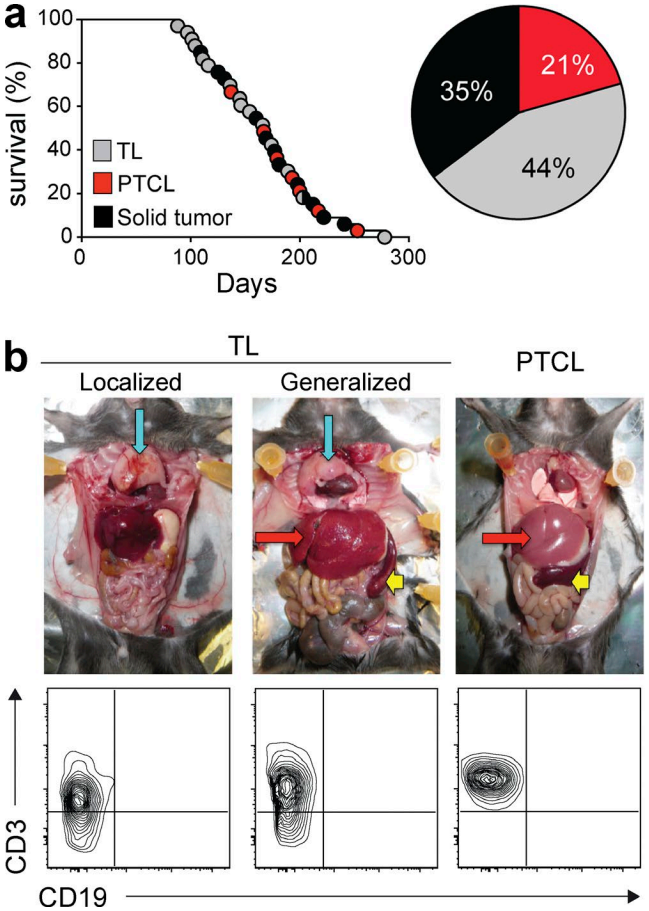


Figure 1. ***p53*$^{-/-}$ mice develop PTCL.** (a) Survival and tumor development spectrum in *p53*$^{-/-}$ mice. Of note, the number of tumors ($n$ = 34) exceeded the total number of mice ($n$ = 33) due to one animal bearing two tumors (i.e., a solid tumor and a lymphoma). (b) Macroscopic and phenotypic characteristics of the three different types of lymphoma encountered in *p53*$^{-/-}$ mice (thymus, blue arrow; spleen, yellow arrow; liver, red arrow). Contour plots were gated on abnormal FSC$^{high}$/SSC$^{high}$ tumor cells recovered from the thymus for TLs and the liver for PTCLs. Data are representative of at least five different TLs and PTCLs.

Until recently, with the notable exception of anaplastic lymphoma kinase (ALK) rearrangement in ALK-positive anaplastic large cell lymphoma, genetic alterations in most PTCL entities were limited to the description of recurrent chromosomal gains and losses without established clinical and biological relevance (Gaulard and de Leval, 2014). However, the advances in deep sequencing technologies have allowed the discovery of recurrent alterations in several PTCLs. These include the recently described *RHOA* G17V hotspot mutation found in up to 70% of angioimmunoblastic T cell lymphomas (Palomero et al., 2014; Sakata-Yanagimoto et al., 2014; Yoo et al., 2014), sometimes in association with *FYN*, *TET2*, *IDH2*, or *DNMT3A* mutations (Quivoron et al., 2011; Cairns et al., 2012; Couronné et al., 2012). Other genomic abnormalities have also been identified, including rearrangements of the

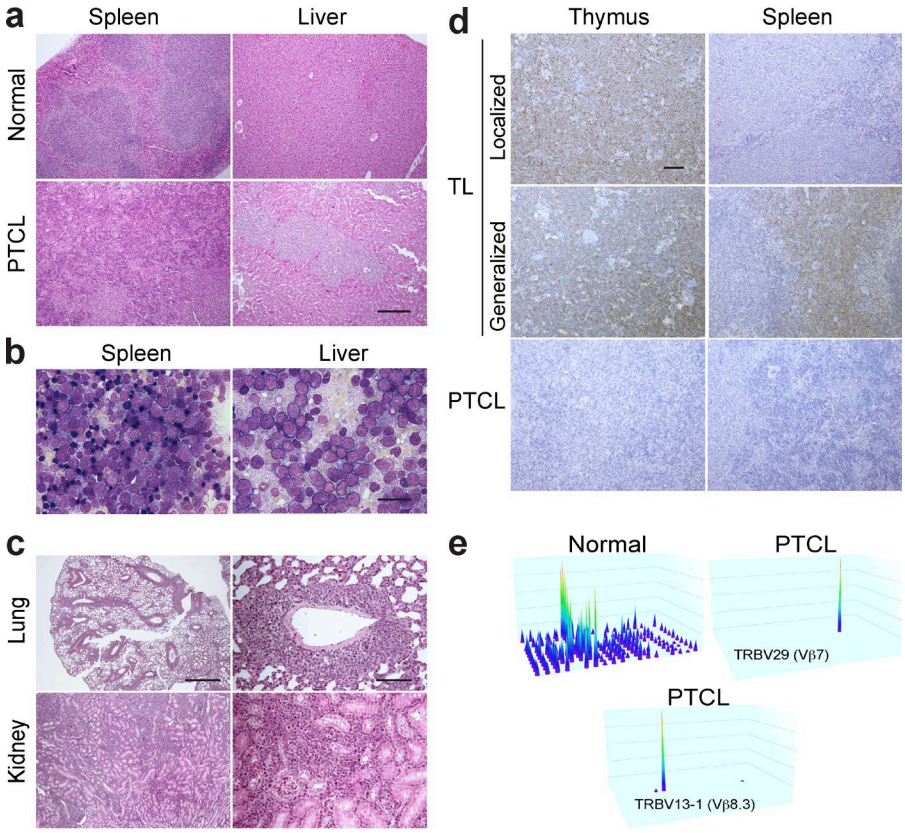


Figure 2. **Histology and clonality of PTCLs.** (a) H&E staining of spleen and liver from normal and PTCL-bearing mice. Bar, 750 µm. Experiments were conducted with five different PTCLs with similar results. (b) H&E staining of spleen and liver appositions from PTCL-bearing mice. Bar, 50 µm. Experiments were conducted with three different PTCLs with similar results. (c) H&E staining of lung and kidney from mice that developed PTCLs. Bars: 500 µm (left); 100 µm (right). Experiments were conducted with five different PTCLs with similar results. (d) TdT staining of formalin-fixed and paraffin-embedded sections from thymi and spleens of representative localized TL, generalized TLs, and PTCLs. Bars, 200 µm. Experiments were conducted with three different PTCLs with similar results. (e) Clonality assessment of the *TRBV* locus (TCRVβ) of spleen cells from one WT mouse and two representative PTCLs mice (out of seven analyzed specimens) by genomic multiplex PCR.

6p25.3 locus, involving *DUSP22* in ALK-positive anaplastic large cell lymphoma (Feldman et al., 2009); *ITK-SYK* rearrangements in some nodal PTCL-not otherwise specified (NOS; Streubel et al., 2006); and *STAT5B* mutations in hepatosplenic T cell lymphomas (HSTLs; Nicolae et al., 2014). Whole-exome sequencing of cutaneous T cell lymphomas and Sézary syndrome have shown that the most prevalent genetic abnormalities include frequent deletions and mutations in chromatin-modifying genes (*TET2*, *DNMT3A*, and *ARID1A*) and in multiple components of the TCR signaling pathway (*PTEN*, *PLCG*1, *PRKCQ*, *CD28*, and *TNFAIP3*), as well as *TP53* (*p53*) mutations or copy number alterations (Cristofoletti et al., 2013;Vaqué et al., 2014; Choi et al., 2015; da Silva Almeida et al., 2015). Inactivating point mutations of *TP53* are particularly rare in other PTCL, but genome-wide analyses have identified structural rearrangements of at least 1 of 5 *TP53*-related genes in 67% of PTCLs (Vasmatzis et al., 2012). Moreover, the cytoplasmic p53 protein is overexpressed in many digestive, cutaneous, and nodal PTCLs (Murray et al., 1995; Lamprecht et al., 2012;Vasmatzis et al., 2012), evocative of a dysfunctional p53 signaling pathway. However, although 70% of $p53^{-/-}$ mice spontaneously develop immature thymic lymphomas (TLs; Donehower et al., 1992; Jacks et al., 1994), little is known about the role of *p53* in mature T cell lymphomagenesis in mice. Although $p53^{-/-}$ mice have been used as a model for immature T cell lymphoma for years, we demonstrate that they are also a suitable model for PTCL development, and uncover a new cellular origin for PTCLs with potential therapeutic application.

## RESULTS

### $p53^{-/-}$ mice develop PTCL

We studied peripheral lymphoma development in $p53^{-/-}$ mice. As expected, all $p53^{-/-}$ mice were dead after 278 d (median survival = 166 d) and approximately two-thirds of the mice developed T cell lymphoma (Fig. 1 a). As previously demonstrated (Donehower et al., 1992; Jacks et al., 1994), most of the mice developed well-known TL (44% of mice) that could be further subdivided into localized TL, where only thymus was macroscopically involved, and generalized TL, where lymphoma cells had spread to liver and spleen (Fig. 1, a and b). However, 21% of mice had massive hepatomegaly and splenomegaly without thymic involvement reminiscent of PTCL (Fig. 1, a and b). In PTCLs, all organs examined (liver, spleen, lung, lymph nodes, bone marrow, and kidney) were characterized by a polymorphic infiltrate of predominantly large cells (Fig. 2, a–c). The architecture of spleen and liver from PTCL mice was nodular and diffuse, with massive cell infiltration leading to the effacement of the normal structure (Fig. 2 a). Negative terminal deoxynucleotidyl transferase (TdT) staining was observed across all samples analyzed, regardless of the organ (thymus, spleen, liver, lymph node, lung, and kidney), as opposed to a strong positive staining in all TLs examined (Fig. 2 d), confirming the post-thymic or mature

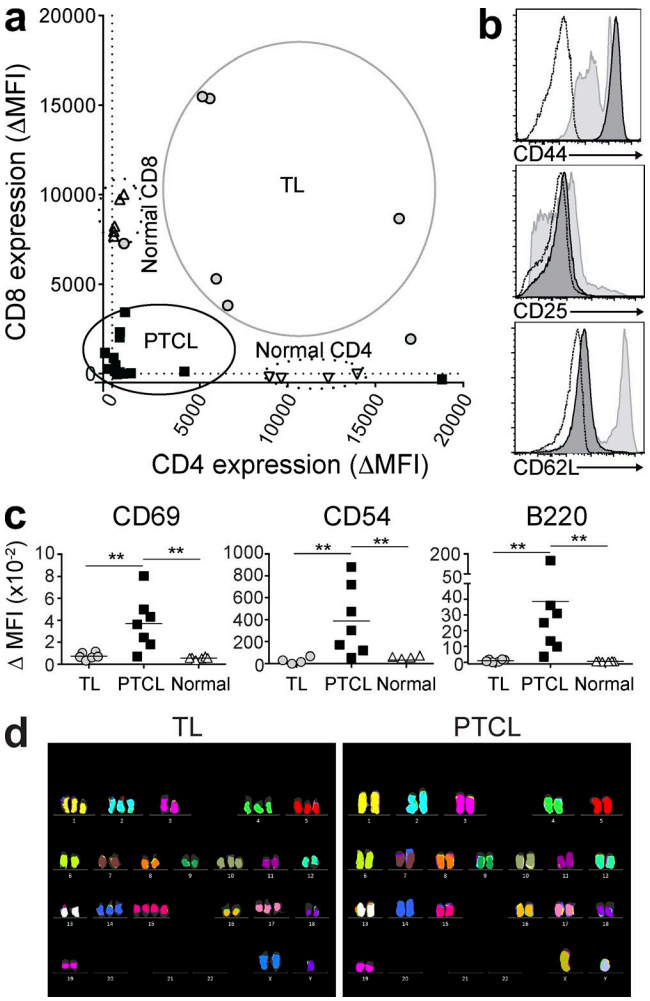


Figure 3. **PTCLs in *p53*$^{-/-}$ mice exhibit features of activated memory-phenotype T cells.** (a) Co-receptor expression in PTCLs compared with TLs, normal CD4$^+$, and CD8$^+$ splenic T cells. (b) Surface staining of PTCLs compared with normal splenic T cells (dark gray shaded histograms indicate PTCLs; light gray shaded histograms indicate normal splenic T cells and dotted lines indicate isotype controls). This staining is representative of all seven PTCLs tested. (c) Expression of activation surface markers in PTCLs compared with TLs and normal splenic T cells. P-values were determined by Mann-Whitney *U* tests. **, $P < 0.01$. (d) Representative M-FISH images of TLs ($n = 2$) and PTCLs ($n = 3$).

origin of these PTCLs. We also demonstrated clonality of the PTCLs using assessment of the variable region of the TCR β chain (*TRBV*) locus by genomic multiplex PCR (Fig. 2 e).

### PTCLs exhibit features of activated memory T cells

Compared with TL and normal CD8$^+$ or CD4$^+$ T cells, all PTCLs had decreased expression of the CD4 and CD8 co-receptor molecules, with most of them being double negative (Fig. 3 a). PTCLs were also CD44$^{hi}$CD25$^-$CD62L$^{lo}$, which suggests an effector–memory T cell phenotype (Fig. 3 b). These staining patterns were consistent across the different organs involved, including spleen, liver, blood, lymph node, and bone marrow (unpublished data). Activation markers, such as CD69, CD54, and B220 (Renno et al., 1998), were significantly up-regulated in PTCLs (Fig. 3 c) compared with TLs and normal T cells. Finally, cytogenetic alterations of PTCLs were examined using multicolor fluorescence in situ hybridization (M-FISH). In sharp contrast to the well-documented aneuploidy observed in TLs (Liu et al., 2004) and to the two TLs that served as positive controls in our study, no clonal translocation or chromosomes number alterations were observed in PTCLs (Fig. 3 d), giving strong support to a distinct pathophysiological transformation process leading to this type of tumor.

### PTCLs originate from invariant NKT (iNKT) cells

Clonality studies of PTCLs revealed a striking Vβ repertoire usage bias with five PTCLs expressing the Vβ7 chain and two the Vβ8 chain (Fig. 2 e and Table 1). Given the strong Vβ8, Vβ7, and Vβ2 repertoire bias that characterizes mouse iNKT cells (Lantz and Bendelac, 1994; Godfrey et al., 2004), we hypothesized that PTCLs might derive from the transformation of these cells. Indeed, a positive staining with CD1d-α-galactosylceramide (αGalCer) tetramer, a specific marker for iNKT cell detection, confirmed this hypothesis (Fig. 4 a). In addition, the transcription factor promyelocytic leukemia zinc finger (PLZF or ZBTB16), which directs the effector program of the iNKT cell lineage, was significantly expressed in these PTCLs (Fig. 4 b). The iNKT cellular origin of PTCLs was further validated by the expression of the invariant Vα14-Jα18 rearrangement of the TCR Vα chain repertoire (Fig. S1). Functionally, iNKT cells are known to rapidly produce high levels of Th1, Th2, or Th17 cytokines upon activation (Kronenberg, 2005; Coquet et al., 2008). All PTCLs expressed IFN-γ and IL-17, either spontaneously or upon activation, but failed to produce IL-4, thereby displaying a Th1 and Th17 cytokine profile (Fig. 4 c). Similar to their normal iNKT cell counterparts (Matsuda et al., 2002), PTCLs expressed CD122 and CD127 and were highly dependent on IL-15 and -7 for their survival in vitro (Fig. 4 d). Finally, PTCLs were characterized by up-regulation of PD-1 and loss of NK1.1 expression, which are all features of activated or anergic iNKT cells (Fig. 4 e; Wilson et al., 2003; Chang et al., 2008). Consistent with the state of anergy, no proliferation, either by [$^3$H]-thymidine incorporation or Cell Trace Violet dilution, could be observed after ex vivo stimulation of PTCLs with anti-CD3/anti-CD28–coated beads or by PMA plus ionomycin in the presence of IL-7 (unpublished data). All these data demonstrate that iNKT cells are the cell-of-origin of these PTCLs, and support a transformation from an activated cell.

### Chronic TCR stimulation drives iNKT cell lymphomagenesis

Because PTCLs expressed features of activated iNKT cells, we explored whether deliberate activation of iNKT cells with repeated injections of heat-killed *Streptococcus pneumonia*

Table 1. **Characteristics of PTCL in p53-deficient mice injected with PBS or bacteria**

| No. | Injections | p53 genotype | TCR | Vα/Vδ chain[a] | Vß/Vγ chain[a] | Co-receptor | CD1d-tetramer binding[b] | PLZF[b] |
|---|---|---|---|---|---|---|---|---|
| 1 | PBS | –/– | αβ | iVα14 | Vβ8.2 | DN | + | + |
| 2 | PBS | –/– | αβ | iVα14 | Vβ7 | DN | + | + |
| 3 | PBS | –/– | αβ | iVα14 | Vβ7 | DN | n.d. | n.d. |
| 4 | PBS | –/– | αβ | iVα14 | Vβ7 | DN | + | + |
| 5 | PBS | –/– | αβ | iVα14 | Vβ7 | $CD8^{lo}$ | n.d. | n.d. |
| 6 | *Spn* | –/– | αβ | iVα14 | Vβ8.2 | $CD8^{lo}$ | + | + |
| 7 | *Spn* | –/– | αβ | iVα14 | Vβ8.3 | DN | + | + |
| 8 | *Spn* | –/– | αβ | iVα14 | Vβ7 | DN | n.d. | n.d. |
| 9 | *Spn* | –/– | αβ | iVα14 | Vβ8.2 | $CD8^{lo}$ | n.d. | n.d. |
| 10 | *Spn* | –/– | αβ | iVα14 | Vβ8.2 | $CD8^{lo}$ | n.d. | n.d. |
| 11 | *Spn* | –/– | αβ | iVα14 | Vβ8.2 | $CD8^{lo}$ | + | + |
| 12 | *Spn* | –/– | αβ | iVα14 | Vβ8 | CD4 | + | + |
| 13 | *Spn* | +/– | αβ | iVα14 | Vβ8.3 | DN | + | + |
| 14 | *Spn* | –/– | γδ | Vδ6.3 | Vγ1.1 | DN | – | + |
| 15 | *Spn* | –/– | γδ | Vδ6.3 | Vγ1.1 | DN | – | + |
| 16 | *Spn* | +/- | γδ | Vδ6.3 | Vγ1.1 | DN | n.d. | n.d. |
| 17 | *E. coli* | –/– | αβ | iVα14 | n.d. | DN | + | n.d. |
| 18 | *E. coli* | –/– | αβ | iVα14 | n.d. | $CD8^{lo}$ | + | n.d. |
| 19 | *E. coli* | –/– | αβ | iVα14 | n.d. | $CD8^{lo}$ | + | n.d. |
| 20 | *E. coli* | –/– | αβ | iVα14 | n.d. | DN | + | n.d. |
| 21 | *E. coli* | –/– | αβ | iVα14 | n.d. | DN | + | n.d. |
| 22 | *E. coli* | –/– | αβ | iVα14 | n.d. | DN | + | n.d. |
| 23 | *E. coli* | –/– | αβ | iVα14 | n.d. | CD4 | + | n.d. |
| 24 | *E. coli* | –/– | αβ | iVα14 | n.d. | DN | + | n.d. |
| 25 | *E. coli* | –/– | αβ | iVα14 | n.d. | CD8lo | + | n.d. |
| 26 | *E. coli* | –/– | αβ | iVα14 | n.d. | n.d. | + | n.d. |
| 27 | *E. coli* | –/– | αβ | iVα14 | n.d. | n.d. | + | n.d. |
| 28 | *E. coli* | –/– | γδ | Vδ6.3 | Vγ1.1 | DN | – | n.d. |

[a]Vα/Vγ and Vß/Vδ chains were determined using either antibody staining and flow cytometry analysis or RT-PCR and nucleotide sequencing of CDR3; iVα14 corresponds to the invariant Vα14 described in iNKT cells.

[b]Assessed by flow cytometry analysis, after fixation and permeabilization for PLZF intracellular staining.

(*Spn*), a bacteria known to express glycolipid antigens that activate iNKT cells through TCR stimulation (Kinjo et al., 2011), could increase the incidence of PTCLs in $p53^{-/-}$ mice. As controls, we chronically injected $p53^{-/-}$ mice with either PBS or heat-killed *Escherichia coli* that do not express iNKT cell antigens. In $p53^{-/-}$ mice, no difference, both in terms of survival or incidence of solid versus hematopoietic tumors, was observed between the PBS-injected group and the *E. coli*– or *Spn*-injected experimental groups (Fig. 5 a). Repeated *Spn* injections shortened survival of $p53^{+/-}$ mice ($P = 0.0045$) by accelerating the development of solid tumors ($P = 0.007$; Fig. 5 a). Importantly in $p53^{-/-}$ mice, PTCLs, unlike other lymphoma subtypes, were overrepresented in the *Spn*-injected group compared with the PBS- and *E. coli*–injected groups ($P < 0.05$; Fig. 5 b). Moreover, although PBS-injected $p53^{+/-}$ mice did not develop PTCLs, chronic injection of heat-killed *Spn* significantly promoted PTCL development in these mice as well ($P = 0.01$; Fig. 5 b). The iNKT cellular origin of these PTCLs was confirmed by CD1d-αGalCer tetramer staining, PLZF expression, and invariant Vα14-Jα18 TCR rearrangements (Table 1). PTCLs expressing Vγ1.1 and Vδ6.3 TCR, a previously reported population of γδ NKT cells (Lees et al., 2001), also arose in *Spn*-injected mice (Table 1).

We next compared the gene expression profile (GEP) of freshly isolated and sorted TLs and PTCLs with normal T and iNKT cells purified from $p53^{-/-}$ mice (either resting or ex vivo activated). Using unsupervised hierarchical clustering, we confirmed that PTCLs were distinct from TLs (Fig. 5 c). Two different clusters were observed that discriminated normal resting T cells, activated T cells, and resting iNKT cells (cluster 1) from tumor cells (cluster 2), with the exception of normal activated iNKT cells that clustered very close to PTCL samples (Fig. 5 c). Thus based on their GEP, PTCLs shared strong similarities with normal activated iNKT cells. To look in more detail at what genes might distinguish PTCLs from normal resting iNKT cells, we performed gene set enrichment analyses (GSEA; Subramanian et al., 2005) using annotated gene sets from the Molecular Signatures Database (Liberzon et al., 2011). Notably, there was a significant down-regulation of genes in the TCR signaling pathway (FDR q-value, 0.011), a phenomenon previously reported in chronically TCR-stimulated T cells (Fig. 5 d). In particular, *CD247* (CD3ζ), *LCK*, and *LAT*, genes known to be down-regulated upon repeated stimulations arising in a context of chronic infection, autoimmunity and inflammation (Baniyash, 2004), were found

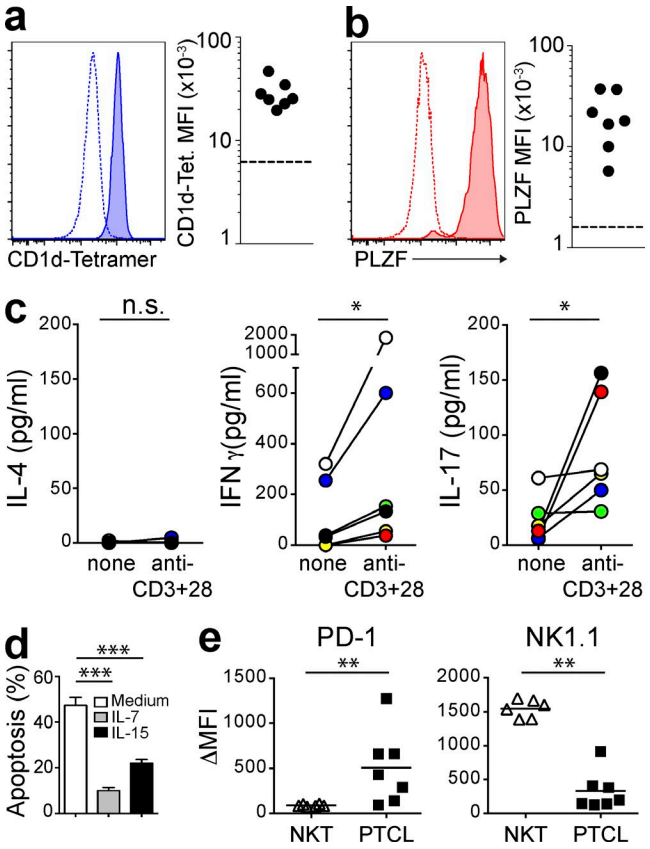


Figure 4. **PTCLs are derived from iNKT cells.** (a) A representative flow cytometry histogram of PTCLs stained with CD1d-αGalCer tetramers is depicted on the left (shaded histogram indicates CD1d-αGalCer tetramer and dashed line represents CD1d-empty tetramer). Sequential gating on abnormal $FSC^{high}/SSC^{high}$ and $CD3^{+}Thy1.2^{+}$ tumor T cells was performed. MFI of CD1d-αGalCer tetramer stainings for different PTCLs are represented on the right. Dotted line represents the highest MFI of CD1d-empty tetramer staining. (b) A representative flow cytometry histogram of intracellular PLZF staining of PTCLs is depicted on the left (shaded histogram indicates PLZF and dashed line isotype control). MFI of PLZF staining for different PTCLs is represented on the right. Dotted line represents the highest MFI of isotype control staining. (c) Cytokines secretion of different PTCLs cultured in the presence or absence of anti-CD3ε– and anti-CD28–coated beads for 24 h. Each color corresponds to one PTCL for IL-4, IL-17, and IFN-γ secretion. P-values were determined by Wilcoxon matched-pairs signed rank test. *, $P < 0.05$ and ns, nonsignificant. (d) Mortality measured by Annexin V staining after culture for 24 h of iNKT lymphoma cells in the absence or presence of IL-7 (10 ng/ml) or IL-15 (10 ng/ml). Data are shown as mean ± SD of one PTCL in quadruplicate and are representative of four experiments performed with different PTCLs (***, $P < 0.001$). (e) Surface expression of PD-1 and NK1.1 in different PTCLs compared with normal iNKT cells. P-values were determined by Mann-Whitney *U* tests. **, $P < 0.01$.

underexpressed compared with normal resting iNKT cells (Fig. 5 e). Furthermore, genes up-regulated by c-Myc were significantly overexpressed (FDR q-value, 0.036) in PTCLs as compared with normal resting iNKT cells (Fig. 6, a and b). *MYC* expression was also significantly up-regulated in PTCLs compared with NKT cells, but more importantly, compared with TLs (Fig. 6 c; $P < 0.05$, Mann-Whitney). Expression of *MYC* is known to be up-regulated after ligation of TCR-CD3, as well as after stimulation with PMA and ionomycin (Lindsten et al., 1988), and is required for TCR-induced proliferation (Guy et al., 2013; Wang et al., 2013). MYC signature was the second most significantly enriched signature when the whole oncogenic (i.e., C6 Molecular Signatures Database) database from the Broad Institute was queried (unpublished data). Together with the down-regulation of genes in the TCR pathway upon chronic stimulation, *MYC* overexpression supports the hypothesis that cell proliferation is mediated by the activation of TCR pathway in PTCLs.

### PTCLs survival depends on TCR–CD1d interactions

A key property of memory T cells generated after acute infection is their ability to persist without antigen encounter (Kaech et al., 2002; Wherry and Ahmed, 2004). Similarly, normal iNKT cells persist in vivo in the absence of TCR–CD1d interactions (Matsuda et al., 2002; Vahl et al., 2013). Conversely, during chronic infections, such as human immunodeficiency virus or hepatitis C virus infections, the survival of antigen-specific memory T cells relies on the persistence of cognate antigens through repeated TCR engagements (Shin et al., 2007). Whether this also applies to chronically activated iNKT cell survival is unknown. To investigate the role of TCR signaling in PTCL survival, we first used cyclosporine A (CsA), a calcineurin inhibitor known to strongly suppress TCR signaling. The viability of PTCL was reduced in a dose-dependent manner i*n vitro* (Fig. 7 a). Furthermore, the in vivo administration of CsA significantly increased the survival of wild type (WT) recipient mice transferred with PTCLs (Fig. 7 b), suggesting that PTCL survival partly relies on TCR signaling pathway. To examine the importance of CD1d-mediated TCR engagement, we transferred PTCLs into $Cd1d^{-/-}$ recipient mice. All $Cd1d^{-/-}$ mice transferred with PTCL survived whereas WT mice did not (Fig. 7 c), suggesting that TCR engagement by CD1d-glycolipid complexes is also a requisite for PTCL survival. On the contrary, CD1d-unrestricted TL did not require TCR–CD1d interaction for survival (Fig. 7 d), thus demonstrating that PTCLs is truly CD1d dependent.

Having established that interrupting the CD1d–TCR interaction is detrimental for PTCL survival, we next evaluated the therapeutic potential of in vivo administration of a blocking CD1d mAb. PTCL cells were transferred into WT C57BL/6 syngeneic recipient mice, followed by blocking CD1d mAb injections twice a week from day 1 (i.e., at the day of PTCL transfer) or day 21 (i.e., at the appearance of the first clinical signs of lymphoma engraftment) until animals had to be sacrificed. Treatment of PTCL-bearing mice with the blocking CD1d mAb, but not with its IgG1 isotype control, delayed PTCL development and significantly increased mouse survival, regardless of the start of the injection (Fig. 7, e and f).

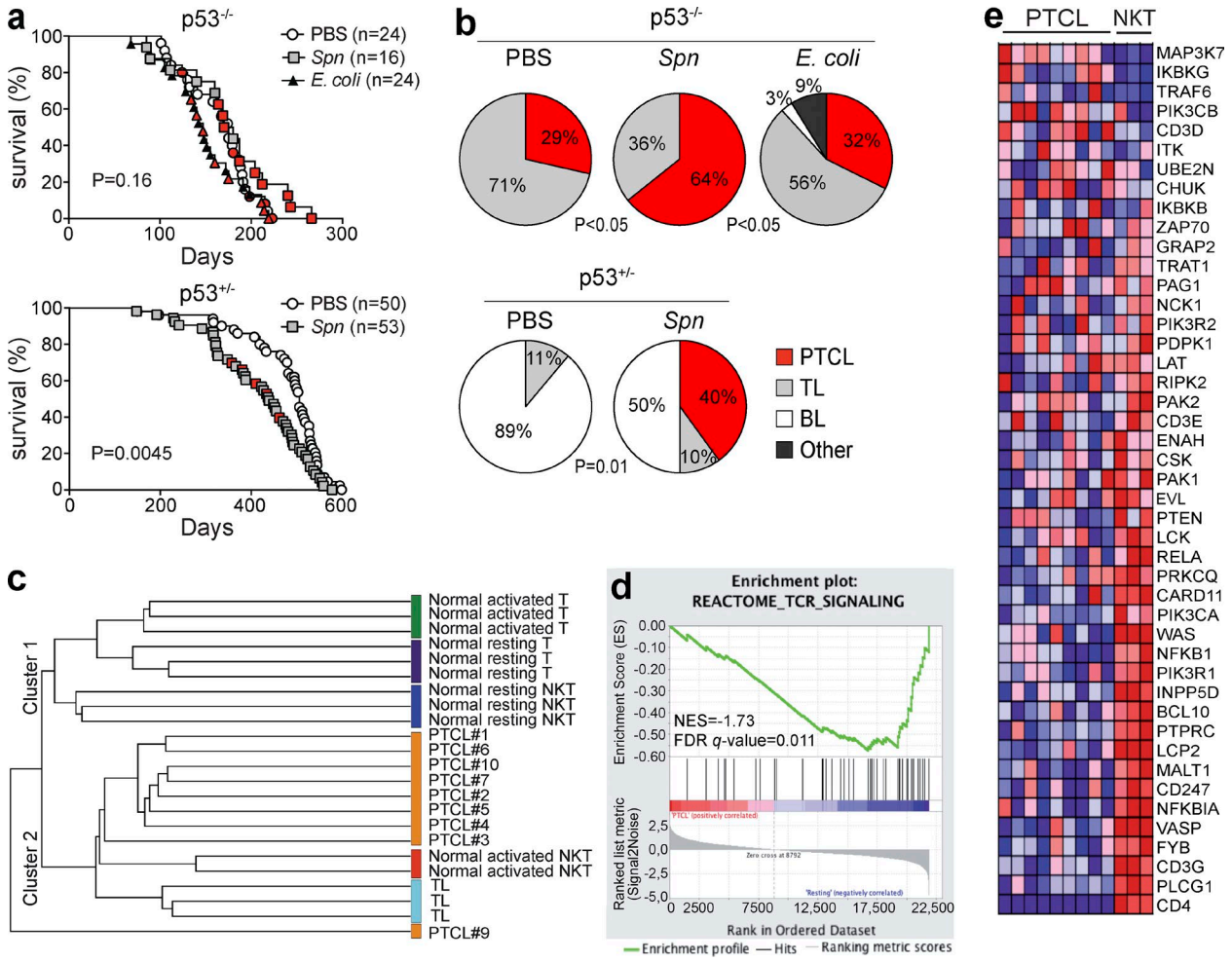


Figure 5. **Chronic stimulation of TCR drives PTCL lymphomagenesis.** (a) Survival curves of PBS-, *Spn*-, and *E. coli*–injected $p53^{-/-}$, and PBS-, and *Spn*-injected $p53^{+/-}$ mice. Red symbols correspond to mice that developed PTCLs. P-values were determined by log-rank test. (b) Lymphoma spectrum in PBS- ($n$ = 24), *Spn*- ($n$ = 16), and *E. coli*–injected ($n$ = 24) $p53^{-/-}$ and PBS- ($n$ = 50) and *Spn*-injected ($n$ = 53) $p53^{+/-}$ mice (solid tumors were not taken into account). P-values were determined by $\chi^2$ test (PTCLs vs. all other lymphomas). In the legend, other corresponds to PTCL originating from conventional T cells. (c) Unsupervised hierarchical clustering based on GEP analysis from nine PTCL samples, TL samples and normal samples from tumor-free $p53^{-/-}$ mice that included resting T and iNKT cells and ex vivo activated T and iNKT cells. The bar on the right of the dendrogram is color-coded according to sample type. (d) GSEA for a set of genes from the TCR signaling pathway. Downward deflection indicates enrichment of the TCR signaling pathway signature in resting iNKT cells from tumor-free $p53^{-/-}$ mice (FDR = 0.011). NES, normalized enrichment score; FDR, false discovery rate. (e) The heat map shows expression of all genes included in the TCR signature.

## Gene expression patterns of murine PTCLs resemble those of specific human T cell malignancies

To find the human counterpart to CD1d-restricted murine PTCL (hereafter referred to as mPTCL), we compared GEP of mPTCLs to those of human PTCLs. GEP data of >400 human PTCL samples from previously published datasets were analyzed (Travert et al., 2012; Iqbal et al., 2014) and compared with the orthologue-based profiles of mPTCLs. Unsupervised hierarchical clustering between murine and human data showed that the closest human entities to mPTCLs were HSTL and T cell prolymphocytic leukemia (T-PLL; unpublished data). Similarly, principal component analysis (PCA) revealed that mPTCLs are closer to human HSTL and T-PLL compared with other human mature T cell malignancies (Fig. 8 a). Genes expressed in NK cells, such as *NCAM1* (CD56) and *KLRD1* (CD94), were found to drive mPTCL and HSTL clustering, as well as chimerin2 (*CHN2*), a gene overexpressed in HSTLs (Finalet Ferreiro et al., 2014) and known to regulate TCR signaling (Siliceo and Mérida, 2009; Fig. 8 b). Among other genes, *BCL7A*, a subunit of the mammalian SWI–SNF complex (Kadoch et al., 2013), and *LEF1*, a transcription factor promoting iNKT cell expansion and differentiation (Carr et al., 2015), drove clustering of mPTCLs with T-PLL (Fig. 8 b). Significantly shared gene expression clusters between human and murine subtypes were illustrated by a heat map based on 82 orthologues among the

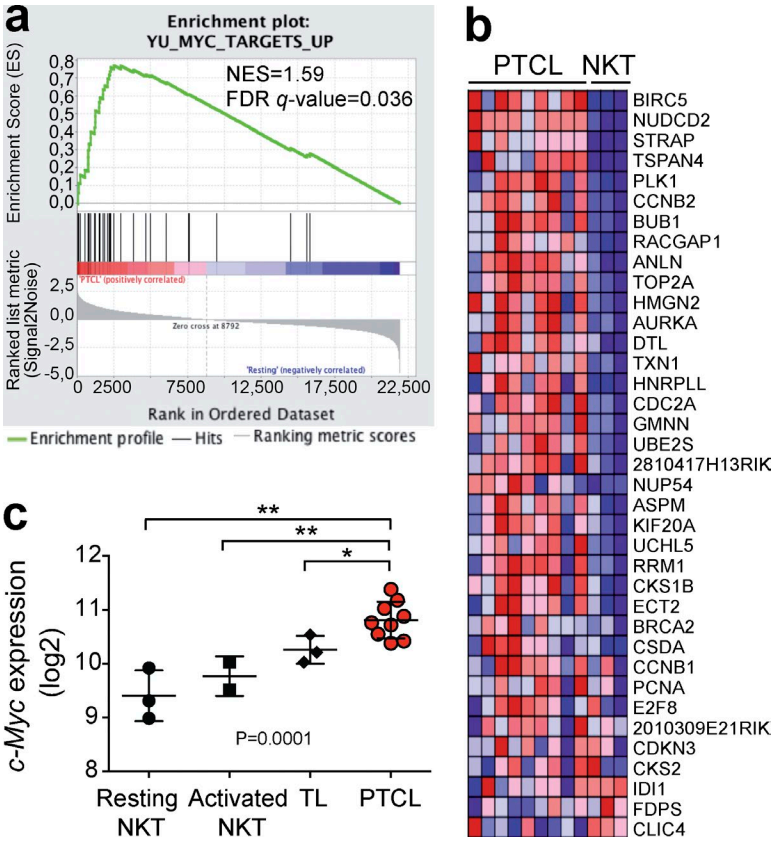


Figure 6. **GEP analysis displays features of c-Myc activation in PTCL.** (a) GSEA analysis of genes up-regulated by c-Myc. Upward deflection of the green line indicates that PTCLs are enriched for genes that are up-regulated by c-Myc, compared with resting iNKT cells; (FDR = 0.036). NES, normalized enrichment score; FDR, false discovery rate. (b) Heat map showing the differential expression of all the genes that constitute the c-Myc signature between PTCLs and resting iNKT cells. (c) *MYC* mRNA up-regulation in PTCLs based on GEP data compared with normal resting and activated iNKT cells, as well as TLs. P-value was determined by Kruskall-Wallis test. P-values between PTCLs and TLs, resting NKT, or activated NKT were determined by Mann-Whitney *U* tests. *, $P < 0.05$; **, $P < 0.01$.

100 genes that best discriminated the human PTCL types from one another (based on an F test; Fig. 8 c and Table S1). Finally, analysis of Gene Ontology (GO) biological processes significantly overexpressed in mPTCL, human HSTL and T-PLL compared with other human entities identified mainly chromosome organization, DNA repair, and epigenetic modifications (Fig. 8 d and Table S1). Conversely, a pronounced down-regulation of immune, cytokine, and inflammatory responses was found. This is consistent with a negative feedback mechanism seen in the context of the chronic antigenic stimulation process suggested in HSTL development (Belhadj et al., 2003). Importantly, removing the murine samples from the analysis led to similar results for HSTL and T-PLL compared with other human lymphomas, implying that the negative feedback loop observed in mPTCLs overdrove GO analysis (unpublished data).

### Vδ1 TCR-expressing human PTCLs are CD1d restricted

HSTLs mostly derive from γδ T cell subsets and exhibit a substantial Vδ1 TCR bias (Belhadj et al., 2003). Several lines of evidence indicate that the surveillance of lipid antigens is not solely restricted to iNKT cells and can be substantially complemented by γδ T cells (Bendelac et al., 2007). Their role may even be more prominent in humans, where iNKT cells are >10-fold less abundant than in mice (Bendelac et al., 2007). Recent reports have demonstrated that, like iNKT cells, a minor population of Vδ1 TCR-expressing T cells recognizes αGalCer or the self-lipid sulfatide presented by the CD1d molecule (Bai et al., 2012; Luoma et al., 2013; Uldrich et al., 2013). We therefore studied whether HSTLs were CD1d-restricted T cell malignancies using human CD1d-loaded tetramers. All Vδ1-expressing lymphoma cells from primary HSTL samples bound human CD1d tetramers loaded with sulfatide but not with αGalCer (Fig. 9 a). Based on the GEP data results, we also tested whether human CD1d tetramers would bind to T-PLL that express αβ TCR. All four T-PLL tested were negative for CD1d tetramer staining, regardless of the glycolipid (Fig. 9 b). This demonstrates that despite their clustering with mPTCLs in terms of GEP, T-PLL is not CD1d restricted. To determine whether the CD1d restriction was dictated by the type of PTCLs or by the nature of the TCR expressed, we examined the binding of human CD1d tetramers to PTCL-NOS and T cell large granular lymphocyte leukemia (T-LGL) expressing Vδ1, Vδ2, or αβ TCR. No binding was observed for Vδ2- and TCRαβ-expressing PTCL-NOS and T-LGL. However, both PTCL-NOS and T-LGL bearing the Vδ1 TCR stained positive for sulfatide-loaded CD1d tetramers, thus confirming a broad CD1d restriction for all tested Vδ1-expressing mature T cell malignancies beyond the GEP similarities (Fig. 9, c and d).

## DISCUSSION

Mice deficient in *p53* are predisposed to develop cancer, such as TL and sarcoma, with 100% cancer-related mortal-

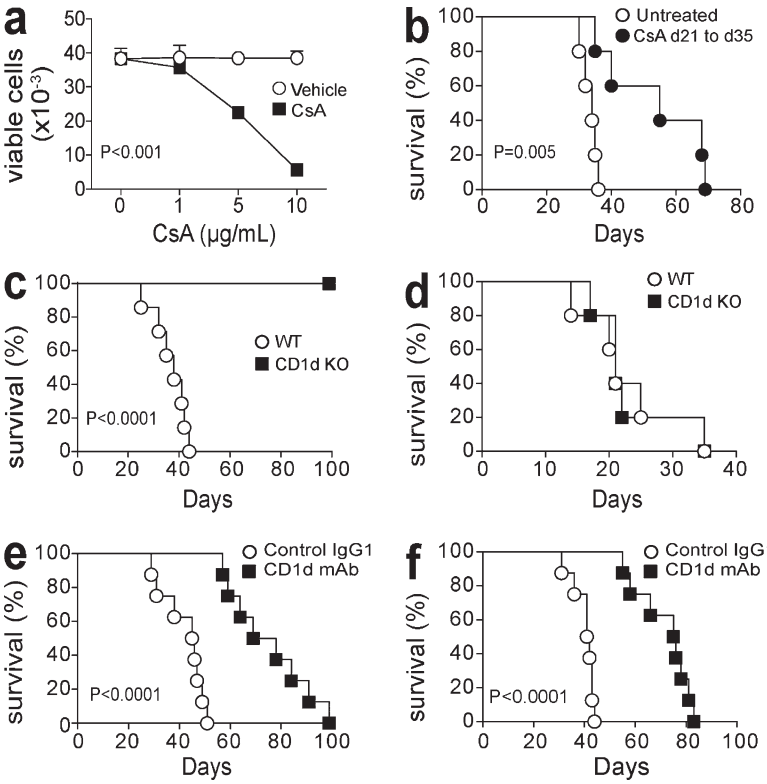


Figure 7. **PTCLs rely on TCR signaling resulting from TCR–CD1d interaction for engraftment and survival.** (a) Cells from PTCLs were cultured in vitro in the presence or absence of increasing concentrations of CsA (or equal concentrations of excipient ethanol, as control vehicle). Data are shown as mean ± SD of one TCRαβ-expressing PTCL in quadruplicate and are representative of four independent experiments performed with four different PTCLs. P-value was determined by two-way ANOVA test. (b) Mice were transferred with $10^6$ PTCL cells, then left untreated ($n$ = 5 mice) or injected i.p. daily with 20 mg/kg of CsA ($n$ = 5 mice) for 2 wk starting from day 21 after transfer (i.e., when abdomen enlargement was clinically detectable). Transfer experiments conducted with three different PTCLs provided similar results. (c) Survival curves of WT and *Cd1d*$^{-/-}$ mice ($n$ = 7) transferred with $10^6$ TCRαβ-expressing PTCL cells. All mice alive at day 100 were sacrificed and showed absence of macroscopic lymphoma development. Experiments were conducted with four different PTCLs with similar results. (d) Survival curves of WT and *Cd1d*$^{-/-}$ mice ($n$ = 5) transferred with $2 \times 10^6$ TL cells. Experiments were conducted with two different TLs with similar results. P-value was determined by log-rank test and was not significant. (e) Survival curves of WT mice transferred with $10^6$ TCRαβ-expressing PTCL cells and injected twice a week by i.p. route with 15 mg/kg of either IgG1 isotype control ($n$ = 8 mice) or blocking CD1d mAb from day 1 ($n$ = 8 mice) and until mice were considered moribund and euthanized. Transfer experiments conducted with three different PTCLs provided similar results. (f) Survival curves of WT mice transferred with $10^6$ TCRαβ-expressing PTCL cells and injected twice a week by i.p. route with 15 mg/kg of either IgG1 control isotype ($n$ = 8 mice) or blocking CD1d mAb from day 21 ($n$ = 8 mice; i.e., when abdomen enlargement was clinically detectable) and until mice were considered moribund and euthanized. Transfer experiments conducted with three different PTCLs provided similar results. P-values in b–f were determined by log-rank test.

ity by ∼300 d (Donehower et al., 1992; Jacks et al., 1994). However, little is known about the role of *p53* in mature T cell lymphomagenesis, although structural rearrangements of at least 1 of 5 *p53*-related genes have been described in 67% of PTCLs (Vasmatzis et al., 2012). In this study, using *p53*$^{-/-}$ mice, we identified a new entity of PTCL that does not originate from conventional T cells but from CD1d-restricted T cells. Most PTCLs arising in *p53*$^{-/-}$ mice were derived from iNKT cells, the most abundant CD1d-restricted T cell subset in mice. The iNKT origin of these PTCLs was demonstrated by CD1d-αGalCer tetramer staining, expression of the transcription factor PLZF or ZBTB16, invariant Vα14-Jα18 rearrangement of the TCR Vα chain, and rapid secretion of Th1 and Th17 cytokines upon activation. Although these lymphomas have never been characterized in previous studies, they were probably described as splenic marginal zone B cell lymphomas because they were defined in *p53*$^{-/-}$ mice as B220- and CD5-positive, two markers expressed by mPTCLs (Ward et al., 1999). Furthermore, whereas many B cell lymphomas were encountered in p53$^{+/-}$ mice, we never identified CD19$^+$ or Ig$^+$ B cell lymphomas in p53$^{-/-}$ mice, whatever the condition (injection with HK *Spn* or controls).

Unlike the well described CD4$^+$CD8$^+$ double positive TLs that develop in p53$^{-/-}$ mice, PTCLs exhibited a normal- or minute-sized thymus with a widespread involvement of all analyzed peripheral organs, including bone marrow, lung, kidney, spleen, and liver, and a lack of immaturity markers, such as TdT. Altogether, these findings led us to consider these lymphomas as postthymic. The liver was predominantly involved in all the diseased mice, consistent with the known preferential localization of normal iNKT cells to the sinusoids of the liver (Bendelac et al., 2007).

Several lines of evidence suggested a contribution of chronic TCR engagement to the development of these PTCLs: (1) the cells showed typical features of activated iNKT cells, such as PD-1 up-regulation and loss of NK1.1 expression; (2) chronic injection of *Spn*, a bacteria known to express glycolipid antigens that activate iNKT cells through TCR stimulation (Kinjo et al., 2011), significantly increased the incidence of PTCLs; (3) GSEA indicated a significant down-regulation of genes in the TCR signaling pathway,

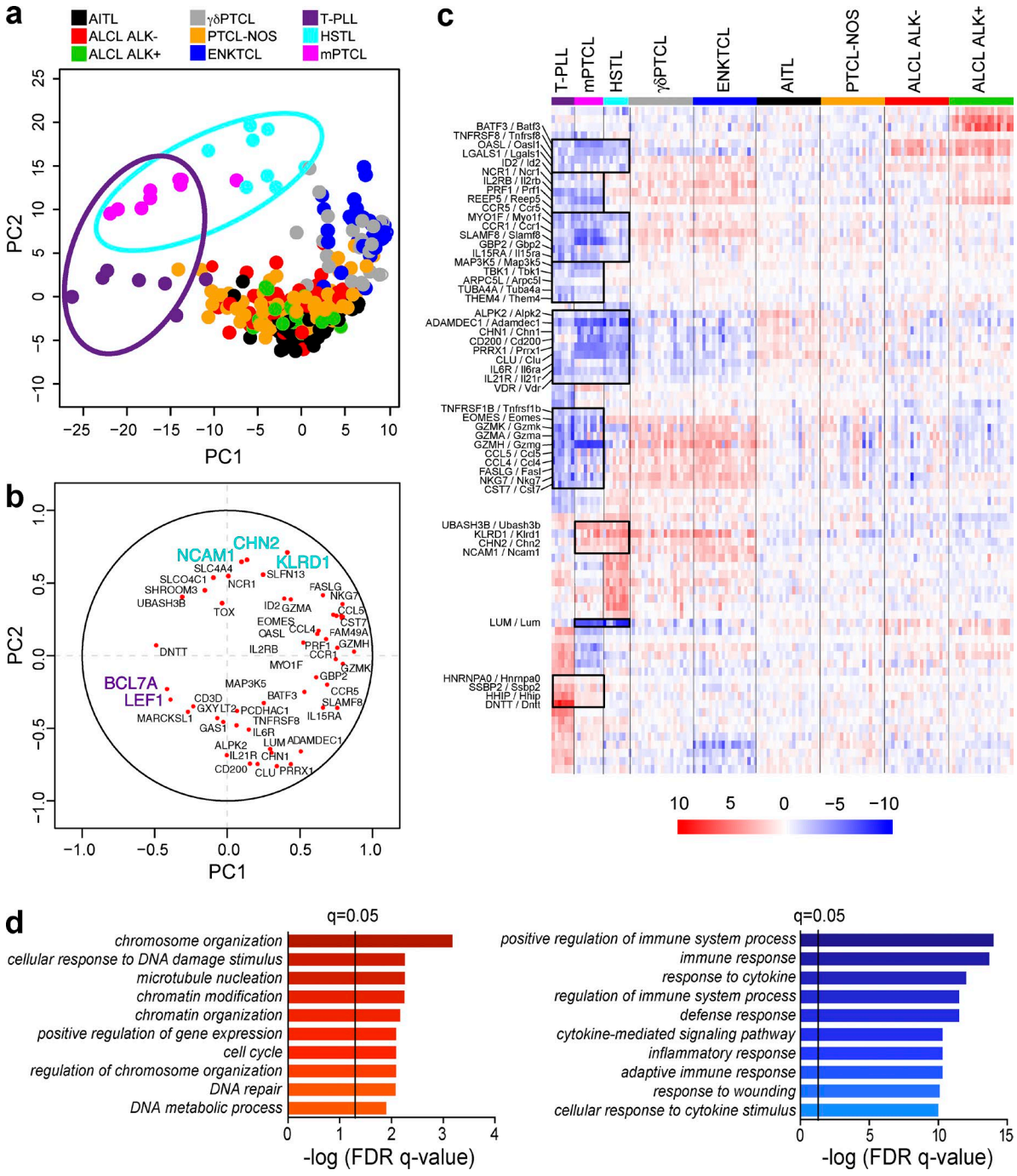


Figure 8. **Gene expression patterns of murine PTCLs resemble those of human HSTL and T-PLL.** (a) Unsupervised PCA showing similarities between murine PTCLs, and human HSTL, and T-PLL compared with other human mature T cell lymphoid malignancies ($n$ = 420 samples). Axes are scaled according to mean-centering and component score distribution. (b) Correlation circle from the unsupervised PCA. Genes highlighted in blue and purple are genes with known function contributing positively to the clustering of murine PTCLs and human HSTLs, and murine PTCLs and human T-PLL, respectively. (c) Heat map of supervised clustering based on GEP analysis from nine murine PTCLs samples and human tumor samples. 82 genes, with orthologues in mouse and human among the 100 genes that best discriminated the human PTCL types from one another (based on an F test), are depicted. The bar above the heat map is color-coded according to the sample type. For better readability, a maximum of only 20 randomly selected human samples per lymphoma subtype are represented (among >400 human samples analyzed). Black boxes indicate clusters of genes overexpressed (red color-coded) or underexpressed (blue color-coded) in mPTCLs and HSTLs or T-PLL clusters compared with other entities. Selected human gene names are shown in capital letters and murine orthologues are shown in lowercase on the left side of the heat map. (d) Representation of the 10 most highly significant subsets among GO biological

previously reported for chronically TCR-stimulated T cells (Baniyash, 2004); (4) CsA, a TCR signaling inhibitor, decreased tumor cell survival in vitro, and prolonged mouse survival after transfer of PTCL cells into recipient mice; (5) engraftments of PTCLs into mice treated with blocking CD1d mAb or into *Cd1d*$^{-/-}$ mice were partially or completely inhibited, respectively, compared with engraftments conducted into WT mice. It could be hypothesized that PTCL cells displayed a poor engraftment in these conditions because they rely on specific CD1d/TCR interactions to survive and/or to proliferate. Indeed, although survival of WT iNKT cells does not require TCR signaling (Vahl et al., 2013) or CD1d expression (Matsuda et al., 2002), it is possible that iNKT cells that have been repeatedly stimulated could become addicted to their cognate antigen and use TCR signaling for long-term maintenance, like exhausted memory CD8$^+$ T cells in chronic infections (Wherry, 2011).

However, if iNKT cell lymphomagenesis is driven by chronic TCR stimulation, spontaneous emergence of PTCLs in *p53*$^{-/-}$ mice raises the question of whether lymphomagenesis could have been driven by environmental factors or self-antigens. Indeed, iNKT cells recognize both self- and microbial lipid-based antigens bound to CD1d. These antigens are widespread in the environment (Wingender et al., 2011) and are also abundant in commensal organisms of the microbiota (Wieland Brown et al., 2013). All PTCLs displayed the same typical features of activated iNKT cells, such as PD-1 up-regulation and loss of NK1.1 expression, lending support to a similar mechanism of transformation in the different groups of mice (spontaneous emergence, PBS-, *E. coli*–, or *Spn*-injected mice). Whether the increased incidence of PTCLs, in the context of chronic pneumococcal stimulation, is only a result of TCR activation triggered by microbial lipid antigen presented by CD1d (Kinjo et al., 2011) or also caused in part by activation by self-antigens presented by CD1d and inflammatory signals from the bacteria remains to be seen. However, no increased incidence of PTCLs in *p53*$^{-/-}$ mice chronically injected with *E. coli,* known to activate iNKT cells through innate cytokine production (Brigl et al., 2011), was observed. This argues that microbial lipid antigens presented by CD1d play a direct role in iNKT cell lymphomagenesis.

Repeated engagements of self- and nonself-antigens, as well as constitutive signaling downstream of the BCR, now emerge as mechanisms by which human B cell type lymphomas might develop and expand (Küppers, 2005; Shaffer et al., 2012). An analogous role of chronic antigenic stimulation via TCR signaling in mature T cell malignancies development is far less documented. However, recent data from mouse models indicated that constitutive TCR signaling by the fusion kinase ITK-SYK drives transformation of mature T cells (Pechloff et al., 2010). In addition, *SNF5*$^{-/-}$ mice develop TCR-dependent PTCLs arising from a peculiar CD8$^+$CD122$^{lo}$ and IL-15–independent memory T cell population (Wang et al., 2011). In humans, a link between chronic stimulation by pathogens or self-antigens and lymphomagenesis has been speculated for T-LGL (Rodríguez-Caballero et al., 2008) and HSTL (Belhadj et al., 2003). GEP analysis showed that murine PTCLs displayed similarities with human HSTL and T-PLL compared with other entities. However, CD1d restriction in human T cell malignancies extended far beyond all Vδ1 TCR-expressing lymphoma cells, identifying for the first time lymphomas deriving from human CD1d-restricted T cells. Interestingly, a recent report described a NKp46$^+$ NKT-like population both in the IL-15 transgenic mouse model of T-LGL and in human T-LGL (Yu et al., 2011). However, this population was not CD1d-restricted like bona fide mouse iNKT cell lymphomas or CD1d-restricted human PTCLs described here.

Aside from CD1d-restricted cells, other unconventional T lymphocytes also recognize nonclassical MHC molecules, such as some of the CD8αα TCRαβ intraepithelial lymphocytes, MR1-specific mucosal invariant T (MAIT) cells (Le Bourhis et al., 2010), and CD1b-restricted human T cells (Van Rhijn et al., 2013). It is tempting to speculate that a previously unsuspected number of human PTCLs could also derive from the transformation of these unconventional T cells. In agreement with this hypothesis, PLZF expression in at least 20% of lymphoma cells has been described in 2 of 26 PTCL-NOS, which were thereafter found to originate from MAIT cells as demonstrated by the TRAV1-2-TRAJ33 TCRα rearrangement (Vα1-2-Jα33; McGregor et al., 2014).

In conclusion, our work describes a previously unrecognized lymphoma entity emerging from CD1d-restricted T cells in mice and humans. Our data highlight the major role of TCR in CD1d-restricted T cell lymphomagenesis and the potential contribution of chronic antigenic stimulation in PTCL etiology, extending to PTCLs the concepts of antigen receptor signaling dependence and chronic stimulation broadly accepted in B cell lymphomagenesis (Suarez et al., 2006). Our present findings, that blocking anti-CD1d mAb delays CD1d-restricted T cell lymphoma engraftment and prolongs the survival of mice, pave the way for the development of a new therapeutic approach for patients with CD1d-restricted PTCLs. In summary, the identification of CD1d-restricted PTCLs in mice and humans alters current classifications of the disease, provides a previously unrecognized animal model, and might lead to promising therapy for patients.

processes when comparing mPTCLs, HSTLs, and T-PLL to other human entities. Processes encompassing up-regulated genes are color-coded in red and processes encompassing down-regulated genes are color-coded in blue. The 300 most differentially up-regulated and down-regulated genes were taken into account for analysis.

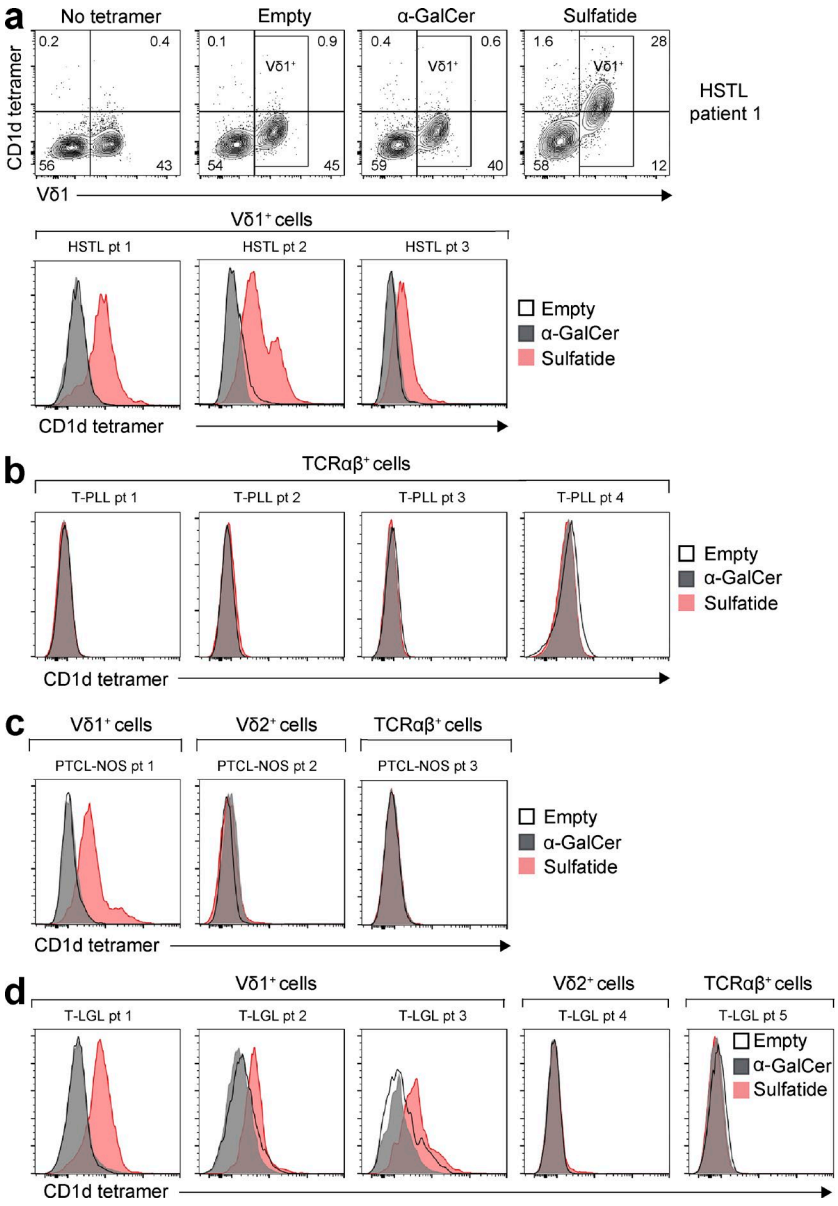


Figure 9. **Vδ1 TCR–expressing human lymphomas are CD1d-restricted PTCLs.** (a) Flow cytometry contour plot analysis showing staining with anti-Vδ1 antibody versus human CD1d-tetramer loaded with αGalCer, sulfatide or unloaded (empty tetramer) of cells from one HSTL patient. Histograms of human CD1d-tetramer stainings gated on Vδ1$^+$ lymphoma cells from all three HSTL patients analyzed are presented below. (b) Flow cytometry histograms of human CD1d-tetramer stainings gated on TCRαβ$^+$ lymphoma cells from four T-PLL patients. (c) Flow cytometry histograms of human CD1d-tetramer stainings gated on Vδ1$^+$, Vδ2$^+$, or TCRαβ$^+$ lymphoma cells from three PTCL-NOS patients. (d) Flow cytometry histograms of human CD1d-tetramer stainings gated on Vδ1$^+$, Vδ2$^+$, or TCRαβ$^+$ leukemic cells from five T-LGL patients.

## MATERIALS AND METHODS

### Mice

*p53*$^{-/-}$ mice (B6.129S2-*Trp53*$^{tm1Tyj}$/J) were purchased from The Jackson Laboratory. *p53*$^{+/-}$ mice were generated by crossing *p53*$^{-/-}$ mice with C57BL/6J WT mice purchased from Charles River Laboratories. *CD3ε*$^{-/-}$ mice were obtained from M. Malissen (Centre d'Immunologie Marseille-Luminy, Marseille, France). *Cd1d*$^{-/-}$ (*Cd1*$^{tm1Gru}$) mice were provided by L. Van Kaer (Howard Hughes Medical Institute, Nashville, TN). All mice were on the C57BL/6J background and were maintained in specific pathogen–free conditions at the Plateau de Biologie Expérimentale de la Souris (Ecole Normale Supérieure de Lyon, Lyon, France). All studies and procedures were performed in accordance with European Union guidelines and approved by the local Animal Ethics Evaluation Committee (CECCAPP).

### Human lymphoma/leukemia cells

Frozen cells were obtained from blood or lymph nodes of lymphoma patients, with informed consent from the patients and review board number 008–09 from the Comité de Protection des Personnes - Ile-de-France IX.

### Flow cytometry analysis

Single-cell suspension prepared from spleen, mesenteric, or mediastinal lymph nodes, liver, and bone marrow were stained with a panel of fluorescently labeled antibodies. Before staining, Fc receptors were blocked for 15 min at 4°C with 24G2 hybridoma supernatant. Data were collected using LSRII and LSR Fortessa flow cytometers (BD) and analyzed with FlowJo software (Tree Star). The following membrane mAbs reactive with murine cells were pur-

chased from BD: CD3ε (145-2C11), CD4 (GK1.5), CD8α (53–6.7), B220 (RA3-6B2), CD69 (H1.2F3), CD62L (MEL-14), CD54 (3E2), CD44 (IM7), CD25 (PC61), TCRβ (H57-597), TCRγδ (GL3), CD5 (53–7.3), CD19 (1D3), CD127 (A7R34), CD122 (TM-β1), NK1.1 (PK136), Vβ5.1+5.2 (MR9-34), Vβ8.1+8.2 (MR5-2), Vβ8.3 (1B3.3) and Vδ6.3/2 (8F4H7B7). Antibodies were conjugated to FITC, PE, PerCP, PerCP-Cy5.5, APC, PE-Cy7, APC-Cy7, or Alexa Fluor 647. PerCP-conjugated anti-Thy1.2 (30-H12) mAb, and PE-conjugated anti-Vγ1.1 (4B2.9) mAb reactive with murine cells was purchased from BioLegend. PE-conjugated anti–PD-1 (J43), PE-conjugated anti-PLZF (Mags.21F7; anti–mouse and –human), and FITC-conjugated anti–human TCRαβ (IP26) were purchased from eBioscience. FITC-conjugated anti–human Vδ1 (TS8.2) and anti–human Vδ2 (15D) were purchased from Thermo Fisher Scientific. For all antibodies, corresponding isotype controls were purchased from the same suppliers. Results expressed in ΔMFI (mean fluorescence intensity) were obtained after subtraction of isotype control MFI from specific marker MFI. PE- and APC-conjugated mouse CD1d-αGalCer tetramers (PBS57) were obtained from the National Institutes of Health Tetramer Core Facility. PE- and APC-conjugated unloaded mouse CD1d tetramers from the same supplier were used as control. Human CD1d tetramers were produced as previously described (Sidobre and Kronenberg, 2002) using αGalCer (Kirin) and sulfatide (Avanti).

### Clonality assessment

PTCL cells from involved spleen or liver were sorted on a FACS Aria sorter (BD). Murine T-lymphocyte repertoire diversity was measured using Immun'Ig tests (ImmunID Technology). Genomic DNA was extracted using standard techniques, and Multi-N-plex PCR reactions were performed using an upstream primer specific to all functional members of a given TRBV family and a downstream primer specific to a given TRBJ segment (international ImMunoGeneTics information system). This assay allows the simultaneous and exhaustive detection of Vβ–Jβ rearrangements in the same reaction. Each Vx–J1, J2, J3, J4, and Jn product was separated as a function of its size, and the Constel'ID software (ImmunID Technologies) was used for further analytical studies, including generation of three-dimensional repertoire illustrations.

### Bacterial culture and injections

The encapsulated serotype 3 WU2 strain of *S. pneumonia*, obtained from A. Fleer (University Medical Center, Utrecht, The Netherlands), was grown in Todd-Hewitt broth supplemented with 0.5% yeast extract to mid-log phase, and then enumerated by plating the suspension on blood agar plates. The *E. coli* strain 25922 from ATCC was grown in LB medium to mid-log phase, and then enumerated by plating the suspension on TBX agar plates. Bacteria were washed twice in PBS and heat-inactivated by a 1-h incubation at 60°C. Aliquots of this suspension were stored at −80°C until use. At the time of injection, $5 \times 10^6$ bacteria were diluted in 200 µl of sterile PBS for intraperitoneal injection, as previously described (Kuranaga et al., 2006). Animal experiments were performed in a biosafety level 2 animal care facility.

### CDR3 sequences of the TCRα and TCRβ chains of PTCL

RNA extracted from cell preparations was converted into cDNA. Samples of cDNA were amplified by PCR for β chain with Vβ- and Cβ-specific primers and for α chain with Vα14 and Cα primers and IQ SuperMix reagents (Bio-Rad Laboratories). PCR were run on a Gene AMP PCR System2700 (Applied Biosystems) with the following conditions: a first cycle at 94°C for 10 min, 35 cycles of 94°C for 3 s, 60°C for 3 s, 72°C for 3 s, and a last cycle at 72°C for 10 min. PCR products were precipitated with ethanol and sequenced using C- and V-specific primers by Cogenics. Primers for constant regions were reverse to transcription orientation: Cβ, 5′-CAGCTCAGCTCCACGTGGTCA GG-3′; Cα, 5′-CTGGGGTAGGTGGCGTT-3′. Primers for the variable regions were specific and in the transcription orientation: Vβ8, 5′-GGCATGGGCTGAGGCTGA TCC-3′; Vβ2, 5′-TCACTGATACGGAGCTGAGGC-3′; Vβ7, 5′-TACAGGGTCTCACGGAAGAAGC-3′; Vα14, 5′-CTAAGCACAGCACGCTGCACA-3′.

### Tumor transplantation and therapeutic in vivo experiments

For transfer experiments, $10^6$ thawed PTCL cells isolated from liver and cryopreserved in 10% DMSO in liquid nitrogen were injected. PTCLs were injected i.v. into syngeneic *Cd1d*$^{-/-}$ and WT mice. For therapeutic trials, 20 mg/kg of CsA (Novartis Pharma) or 15 mg/kg of blocking CD1d mAbs (clone HB323; BioXcell) diluted in 200 µl of PBS were injected daily or twice a week, respectively, from day 1 after transfer of PTCLs or when tumors became clinically apparent in the transplant-recipient mice (i.e., at day 21). All groups of mice were age and sex matched.

### Immunostaining

For immunohistochemistry, thymus, spleen, liver, kidney, lung, and mesenteric or mediastinal lymph nodes were fixed in 10% formaldehyde and paraffin embedded. 4-µm-thick sections were stained with hematoxylin and eosin (H&E) or immunostained with anti-TdT (A3524; Dako). For cytology, fresh tissue appositions were obtained by touch imprints of spleen and liver. Sections and appositions were viewed using a Leica DMR microscope and images were captured with a digital camera (DXM 1200C; Nikon).

### Microarray analysis

**Cell sorting.** Thymic and PCTL tumoral cells from thymus or liver, respectively, were sorted on a FACSAria sorter (BD). Purity was consistently >98%. Sorted normal iNKT cells from liver and normal T lymphocytes pooled from spleen and mesenteric lymph nodes from age-matched WT animals were used as controls. For normal iNKT cell and T cell activation,

anti-CD3/anti-CD28–coated beads (Invitrogen) were used at a 1:1 bead-to-cell ratio in 3-d cultures.

**Target labeling.** Total RNA was extracted using TRIzol-Reagent (Invitrogen) and was amplified by two rounds of in vitro transcription (IVT) using an ExpressArt C&E mRNA amplification nano kit (AmpTec GmbH). During the second IVT amplification, RNA was biotin-labeled using BioArray HighYield RNA Transcript Labeling kit (Enzo Life Sciences). Before amplification, spikes of synthetic mRNA (GeneChip Eukaryotic Poly-A RNA Controls; Affymetrix) at different concentrations were added to all samples; these positive controls were used to ascertain the quality of the process. Biotinylated antisense cRNA quantification was performed with Nanodrop 1000 (Nanodrop) and quality checked with Agilent 2100 Bioanalyzer (Agilent Technologies).

**Array hybridizations, scanning, and normalization.** Hybridization was performed following the Affymetrix protocol. In brief, 15 µg of labeled cRNA was fragmented and denatured in hybridization buffer, and then 10 µg was hybridized on GeneChip Mouse Genome 430 2.0 array (Affymetrix) for 16 h at 45°C with constant mixing by rotation at 60 rpm in the Hybridization Oven 640 (Affymetrix). After hybridization, arrays were washed and stained with streptavidin-phycoerythrin (GeneChip Hybridization Wash and Stain kit) in the Fluidics Station 450 (Affymetrix) according to the manufacturer's instruction. The arrays were read with a confocal laser (GeneChip Scanner 3000 7G; Affymetrix). The CEL files were generated using the Affymetrix GeneChip Command Console software 3.0. The obtained data were normalized with Affymetrix Expression Console software using MAS5 statistical algorithm.

GSEA was performed using the publicly available desktop application from the Broad Institute after normalization with Affymetrix Expression Console software using MAS5 statistical algorithm. Affymetrix CEL files from mouse samples were also analyzed in R using the Bioconductor. Raw probe signals were background-corrected using the maximum likelihood estimation of the normal-exponential mixture model, and normalized using the variance-stabilization transformation, followed by a quantile normalization. Summarization was performed using the median-polish version 17.1 of the Entrez Gene-based reannotated chip description file. Murine microarray data have been deposited into the Gene Expression omnibus (GEO) database under accession no. GSE63264. GEP from human samples for hierarchical clustering, PCA, and GO analyses were collected from ArrayExpress accession nos. E-TABM-702, E-TABM-783, and E-TABM-638, and GEO accession nos. GSE19067, GSE58445, GSE19069, and GSE6338. The various human GEP datasets were normalized in BRB-ArrayTools v4.5.0 Beta 2 using default settings, exported, combined, and batch corrected via Combat. The batch corrected datasets were reimported into BRB-ArrayTools, but not renormalized. The mouse expression matrix was combined with the human expression matrix, pairing orthologue genes based on the information in version 68 of HomoloGene. In the PCA analysis, distance between individual samples was depicted according to the first two principal components. First and second principal components accounted for >40% of the total variance. For analysis of GO biological processes, the 300 most differentially up-regulated or down-regulated genes between groups of entities were considered.

### IL-7, IL-15m, and CsA in vitro experiments

PTCL viability was assessed after 24 h of culture in medium alone or in medium supplemented with 10 ng/ml of IL-7 (R&D Systems) or IL-15 (R&D Systems), or with increasing concentrations of CsA (Sigma-Aldrich). Viability was assessed by PTCL staining with FITC-conjugated Annexin V at the indicated time.

### M-FISH

M-FISH was performed on chromosome spreads obtained from fixed-cell material and prepared using standard cytogenetic protocols. A mix of 21 labeled painting probes specific to the different mouse chromosomes was used (MetaSystems). Experiments were performed according to the manufacturer's protocols. Metaphase spreads were analyzed using a fluorescence microscope (Axioplan II; ZEISS) equipped with appropriate filters (DAPI, FITC, Spectrum Orange, TRITC, Cy5, and DEAC). Images were captured and processed using the ISIS/mFISH imaging system (Metasystems).

### Statistical analyses

All analyses were performed using Prism (GraphPad Software) version 6.0. In all figures, histograms represent mean and error bars represent SD. Comparisons were made with the $\chi^2$ test or the Fisher's exact test for categorical variables, and with Mann-Whitney nonparametric test for continuous parameters. Survival curves were constructed with the Kaplan-Meier method and survival distributions were compared by the log-rank test. All tests were two-sided and p-values of $<0.05$ were considered statistically significant.

### Online supplemental material

Fig. S1 shows CDR3 nucleotide and amino acid sequences of the TCR Vα rearrangements of PTCL. Table S1 shows gene ontology terms most strongly up-regulated and down-regulated in mPTCL, human HSTL, and T-PLL compared with other human PTCL entities. Online supplemental material is available at http://www.jem.org/cgi/content/full/jem.20150794/DC1.

## ACKNOWLEDGMENTS

We thank the National Institutes of Health Tetramer Facility for mouse CD1d tetramers; T. Andrieu and S. Dussurgey (SFR BioSciences – UMS3444/US8) for technical assistance with flow cytometry and cell sorting; N. Aguilera and J.-F. Henry (PBES, SFR BioSciences Gerland – UMS3444/US8) for help at the animal care facility; S. Croze, A.

Besse (ProfileXpert), and S. Tymen (Altrabio) for assistance in GEP analysis; L. Moro-Sobilot for iconography assistance; and V. Bachy for discussions and critical reading of the manuscript.

L. Genestier was supported by Institut National de la Santé et de la Recherche Médicale, CLARA "program Oncostarter", Plan Cancer 2009-2013, the Institut Carnot CALYM granted by the French National Research Agency, grants from "Ligue contre le Cancer-CD69 and CD26," and a grant from the ARC foundation. M. Herling was supported by a Deutsche Forschungsgemeinschaft grant as part of the FOR1961 (HE-3553/4-1).

The authors declare no competing financial interests.

**Submitted: 7 May 2015**

**Accepted: 25 February 2016**

## REFERENCES

Bai, L., D. Picard, B. Anderson, V. Chaudhary, A. Luoma, B. Jabri, E.J. Adams, P.B. Savage, and A. Bendelac. 2012. The majority of CD1d-sulfatide-specific T cells in human blood use a semiinvariant Vδ1 TCR. *Eur. J. Immunol.* 42:2505–2510. http://dx.doi.org/10.1002/eji.201242531

Baniyash, M. 2004. TCR zeta-chain downregulation: curtailing an excessive inflammatory immune response. *Nat. Rev. Immunol.* 4:675–687. http://dx.doi.org/10.1038/nri1434

Belhadj, K., F. Reyes, J.P. Farcet, H. Tilly, C. Bastard, R. Angonin, E. Deconinck, F. Charlotte, V. Leblond, E. Labouyrie, et al. 2003. Hepatosplenic gammadelta T-cell lymphoma is a rare clinicopathologic entity with poor outcome: report on a series of 21 patients. *Blood.* 102:4261–4269. http://dx.doi.org/10.1182/blood-2003-05-1675

Bendelac, A., P.B. Savage, and L. Teyton. 2007. The biology of NKT cells. *Annu. Rev. Immunol.* 25:297–336. http://dx.doi.org/10.1146/annurev.immunol.25.022106.141711

Brigl, M., R.V. Tatituri, G.F. Watts, V. Bhowruth, E.A. Leadbetter, N. Barton, N.R. Cohen, F.F. Hsu, G.S. Besra, and M.B. Brenner. 2011. Innate and cytokine-driven signals, rather than microbial antigens, dominate in natural killer T cell activation during microbial infection. *J. Exp. Med.* 208:1163–1177. http://dx.doi.org/10.1084/jem.20102555

Cairns, R.A., J. Iqbal, F. Lemonnier, C. Kucuk, L. de Leval, J.P. Jais, M. Parrens, A. Martin, L. Xerri, P. Brousset, et al. 2012. IDH2 mutations are frequent in angioimmunoblastic T-cell lymphoma. *Blood.* 119:1901–1903. http://dx.doi.org/10.1182/blood-2011-11-391748

Carr, T., V. Krishnamoorthy, S. Yu, H.H. Xue, B.L. Kee, and M. Verykokakis. 2015. The transcription factor lymphoid enhancer factor 1 controls invariant natural killer T cell expansion and Th2-type effector differentiation. *J. Exp. Med.* 212:793–807. http://dx.doi.org/10.1084/jem.20141849

Chang, W.S., J.Y. Kim, Y.J. Kim, Y.S. Kim, J.M. Lee, M. Azuma, H. Yagita, and C.Y. Kang. 2008. Cutting edge: Programmed death-1/programmed death ligand 1 interaction regulates the induction and maintenance of invariant NKT cell anergy. *J. Immunol.* 181:6707–6710. http://dx.doi.org/10.4049/jimmunol.181.10.6707

Choi, J., G. Goh, T. Walradt, B.S. Hong, C.G. Bunick, K. Chen, R.D. Bjornson, Y. Maman, T. Wang, J. Tordoff, et al. 2015. Genomic landscape of cutaneous T cell lymphoma. *Nat. Genet.* 47:1011–1019. http://dx.doi.org/10.1038/ng.3356

Coquet, J.M., S. Chakravarti, K. Kyparissoudis, F.W. McNab, L.A. Pitt, B.S. McKenzie, S.P. Berzins, M.J. Smyth, and D.I. Godfrey. 2008. Diverse cytokine production by NKT cell subsets and identification of an IL-17–producing $CD4^{-}NK1.1^{-}$ NKT cell population. *Proc. Natl. Acad. Sci. USA.* 105:11287–11292. http://dx.doi.org/10.1073/pnas.0801631105

Couronné, L., C. Bastard, and O.A. Bernard. 2012. TET2 and DNMT3A mutations in human T-cell lymphoma. *N. Engl. J. Med.* 366:95–96. http://dx.doi.org/10.1056/NEJMc1111708

Cristofoletti, C., M.C. Picchio, C. Lazzeri, V. Tocco, E. Pagani, A. Bresin, B. Mancini, F. Passarelli, A. Facchiano, E. Scala, et al. 2013. Comprehensive analysis of PTEN status in Sezary syndrome. *Blood.* 122:3511–3520. http://dx.doi.org/10.1182/blood-2013-06-510578

da Silva Almeida, A.C., F. Abate, H. Khiabanian, E. Martinez-Escala, J. Guitart, C.P. Tensen, M.H. Vermeer, R. Rabadan, A. Ferrando, and T. Palomero. 2015. The mutational landscape of cutaneous T cell lymphoma and Sézary syndrome. *Nat. Genet.* 47:1465–1470. http://dx.doi.org/10.1038/ng.3442

de Leval, L., D.S. Rickman, C. Thielen, A. Reynies, Y.L. Huang, G. Delsol, L. Lamant, K. Leroy, J. Brière, T. Molina, et al. 2007. The gene expression profile of nodal peripheral T-cell lymphoma demonstrates a molecular link between angioimmunoblastic T-cell lymphoma (AITL) and follicular helper T (TFH) cells. *Blood.* 109:4952–4963. http://dx.doi.org/10.1182/blood-2006-10-055145

Donehower, L.A., M. Harvey, B.L. Slagle, M.J. McArthur, C.A. Montgomery Jr., J.S. Butel, and A. Bradley. 1992. Mice deficient for p53 are developmentally normal but susceptible to spontaneous tumours. *Nature.* 356:215–221. http://dx.doi.org/10.1038/356215a0

Feldman, A.L., M. Law, E.D. Remstein, W.R. Macon, L.A. Erickson, K.L. Grogg, P.J. Kurtin, and A. Dogan. 2009. Recurrent translocations involving the IRF4 oncogene locus in peripheral T-cell lymphomas. *Leukemia.* 23:574–580. http://dx.doi.org/10.1038/leu.2008.320

Finalet Ferreiro, J., L. Rouhigharabaei, H. Urbankova, J.A. van der Krogt, L. Michaux, S. Shetty, L. Krenacs, T. Tousseyn, P. De Paepe, A. Uyttebroeck, et al. 2014. Integrative genomic and transcriptomic analysis identified candidate genes implicated in the pathogenesis of hepatosplenic T-cell lymphoma. *PLoS One.* 9:e102977. http://dx.doi.org/10.1371/journal.pone.0102977

Gaulard, P., and L. de Leval. 2014. Pathology of peripheral T-cell lymphomas: where do we stand? *Semin. Hematol.* 51:5–16. http://dx.doi.org/10.1053/j.seminhematol.2013.11.003

Godfrey, D.I., H.R. MacDonald, M. Kronenberg, M.J. Smyth, and L.Van Kaer. 2004. NKT cells: what's in a name? *Nat. Rev. Immunol.* 4:231–237. http://dx.doi.org/10.1038/nri1309

Guy, C.S., K.M. Vignali, J. Temirov, M.L. Bettini, A.E. Overacre, M. Smeltzer, H. Zhang, J.B. Huppa, Y.H. Tsai, C. Lobry, et al. 2013. Distinct TCR signaling pathways drive proliferation and cytokine production in T cells. *Nat. Immunol.* 14:262–270. http://dx.doi.org/10.1038/ni.2538

Iqbal, J., G. Wright, C. Wang, A. Rosenwald, R.D. Gascoyne, D.D. Weisenburger, T.C. Greiner, L. Smith, S. Guo, R.A. Wilcox, et al. Lymphoma Leukemia Molecular Profiling Project and the International Peripheral T-cell Lymphoma Project. 2014. Gene expression signatures delineate biological and prognostic subgroups in peripheral T-cell lymphoma. *Blood.* 123:2915–2923. http://dx.doi.org/10.1182/blood-2013-11-536359

Jacks, T., L. Remington, B.O. Williams, E.M. Schmitt, S. Halachmi, R.T. Bronson, and R.A. Weinberg. 1994. Tumor spectrum analysis in p53-mutant mice. *Curr. Biol.* 4:1–7. http://dx.doi.org/10.1016/S0960-9822(00)00002-6

Kadoch, C., D.C. Hargreaves, C. Hodges, L. Elias, L. Ho, J. Ranish, and G.R. Crabtree. 2013. Proteomic and bioinformatic analysis of mammalian SWI/SNF complexes identifies extensive roles in human malignancy. *Nat. Genet.* 45:592–601. http://dx.doi.org/10.1038/ng.2628

Kaech, S.M., E.J. Wherry, and R. Ahmed. 2002. Effector and memory T-cell differentiation: implications for vaccine development. *Nat. Rev. Immunol.* 2:251–262. http://dx.doi.org/10.1038/nri778

Kinjo, Y., P. Illarionov, J.L. Vela, B. Pei, E. Girardi, X. Li, Y. Li, M. Imamura, Y. Kaneko, A. Okawara, et al. 2011. Invariant natural killer T cells recognize glycolipids from pathogenic Gram-positive bacteria. *Nat. Immunol.* 12:966–974. http://dx.doi.org/10.1038/ni.2096

Kronenberg, M. 2005. Toward an understanding of NKT cell biology: progress and paradoxes. *Annu. Rev. Immunol.* 23:877–900. http://dx.doi.org/10.1146/annurev.immunol.23.021704.115742

Küppers, R. 2005. Mechanisms of B-cell lymphoma pathogenesis. *Nat. Rev. Cancer.* 5:251–262. http://dx.doi.org/10.1038/nrc1589

Kuranaga, N., M. Kinoshita, T. Kawabata, Y. Habu, N. Shinomiya, and S. Seki. 2006. Interleukin-18 protects splenectomized mice from lethal Streptococcus pneumoniae sepsis independent of interferon-gamma by inducing IgM production. *J. Infect. Dis.* 194:993–1002. http://dx.doi.org/10.1086/507428

Lamprecht, B., S. Kreher, M. Möbs, W. Sterry, B. Dörken, M. Janz, C. Assaf, and S. Mathas. 2012. The tumour suppressor p53 is frequently nonfunctional in Sézary syndrome. *Br. J. Dermatol.* 167:240–246. http://dx.doi.org/10.1111/j.1365-2133.2012.10918.x

Lantz, O., and A. Bendelac. 1994. An invariant T cell receptor alpha chain is used by a unique subset of major histocompatibility complex class I-specific CD4+ and CD4-8- T cells in mice and humans. *J. Exp. Med.* 180:1097–1106. http://dx.doi.org/10.1084/jem.180.3.1097

Le Bourhis, L., E. Martin, I. Péguillet, A. Guihot, N. Froux, M. Coré, E. Lévy, M. Dusseaux, V. Meyssonnier, V. Premel, et al. 2010. Antimicrobial activity of mucosal-associated invariant T cells. *Nat. Immunol.* 11:701–708. http://dx.doi.org/10.1038/ni.1890

Lees, R.K., I. Ferrero, and H.R. MacDonald. 2001. Tissue-specific segregation of TCR gamma delta+ NKT cells according to phenotype TCR repertoire and activation status: parallels with TCR $\alpha\beta^+$ NKT cells. *Eur. J. Immunol.* 31:2901–2909. http://dx.doi.org/10.1002/1521-4141(2001010)31:10<2901::AID-IMMU2901>3.0.CO;2-#

Liberzon, A., A. Subramanian, R. Pinchback, H. Thorvaldsdóttir, P. Tamayo, and J.P. Mesirov. 2011. Molecular signatures database (MSigDB) 3.0. *Bioinformatics.* 27:1739–1740. http://dx.doi.org/10.1093/bioinformatics/btr260

Lindsten, T., C.H. June, and C.B. Thompson. 1988. Multiple mechanisms regulate c-myc gene expression during normal T cell activation. *EMBO J.* 7:2787–2794.

Liu, G., J.M. Parant, G. Lang, P. Chau, A. Chavez-Reyes, A.K. El-Naggar, A. Multani, S. Chang, and G. Lozano. 2004. Chromosome stability, in the absence of apoptosis, is critical for suppression of tumorigenesis in Trp53 mutant mice. *Nat. Genet.* 36:63–68. http://dx.doi.org/10.1038/ng1282

Luoma, A.M., C.D. Castro, T. Mayassi, L.A. Bembinster, L. Bai, D. Picard, B. Anderson, L. Scharf, J.E. Kung, L.V. Sibener, et al. 2013. Crystal structure of Vδ1 T cell receptor in complex with CD1d-sulfatide shows MHC-like recognition of a self-lipid by human γδ T cells. *Immunity.* 39:1032–1042. http://dx.doi.org/10.1016/j.immuni.2013.11.001

Matsuda, J.L., L. Gapin, S. Sidobre, W.C. Kieper, J.T. Tan, R. Ceredig, C.D. Surh, and M. Kronenberg. 2002. Homeostasis of V alpha 14i NKT cells. *Nat. Immunol.* 3:966–974. http://dx.doi.org/10.1038/ni837

McGregor, S., A. Shah, G. Raca, M.K. Mirza, S.M. Smith, J. Anastasi, J.W. Vardiman, E. Hyjek, and S. Gurbuxani. 2014. PLZF staining identifies peripheral T-cell lymphomas derived from innate-like T-cells with TRAV1-2-TRAJ33 TCR-α rearrangement. *Blood.* 123:2742–2743. http://dx.doi.org/10.1182/blood-2014-02-555482

Murray, A., E.C. Cuevas, D.B. Jones, and D.H. Wright. 1995. Study of the immunohistochemistry and T cell clonality of enteropathy-associated T cell lymphoma. *Am. J. Pathol.* 146:509–519.

Nicolae, A., L. Xi, S. Pittaluga, Z. Abdullaev, S.D. Pack, J. Chen, T.A. Waldmann, E.S. Jaffe, and M. Raffeld. 2014. Frequent STAT5B mutations in γδ hepatosplenic T-cell lymphomas. *Leukemia.* 28:2244–2248. http://dx.doi.org/10.1038/leu.2014.200

Palomero, T., L. Couronné, H. Khiabanian, M.Y. Kim, A. Ambesi-Impiombato, A. Perez-Garcia, Z. Carpenter, F. Abate, M. Allegretta, J.E. Haydu, et al. 2014. Recurrent mutations in epigenetic regulators, RHOA and FYN kinase in peripheral T cell lymphomas. *Nat. Genet.* 46:166–170. http://dx.doi.org/10.1038/ng.2873

Pechloff, K., J. Holch, U. Ferch, M. Schweneker, K. Brunner, M. Kremer, T. Sparwasser, L. Quintanilla-Martinez, U. Zimber-Strobl, B. Streubel, et al. 2010. The fusion kinase ITK-SYK mimics a T cell receptor signal and drives oncogenesis in conditional mouse models of peripheral T cell lymphoma. *J. Exp. Med.* 207:1031–1044. http://dx.doi.org/10.1084/jem.20092042

Quivoron, C., L. Couronné, V. Della Valle, C.K. Lopez, I. Plo, O. Wagner-Ballon, M. Do Cruzeiro, F. Delhommeau, B. Arnulf, M.-H. Stern, et al. 2011. TET2 inactivation results in pleiotropic hematopoietic abnormalities in mouse and is a recurrent event during human lymphomagenesis. *Cancer Cell.* 20:25–38. http://dx.doi.org/10.1016/j.ccr.2011.06.003

Renno, T., A. Attinger, D. Rimoldi, M. Hahne, J. Tschopp, and H.R. MacDonald. 1998. Expression of B220 on activated T cell blasts precedes apoptosis. *Eur. J. Immunol.* 28:540–547. http://dx.doi.org/10.1002/(SICI)1521-4141(199802)28:02<540::AID-IMMU540>3.0.CO;2-Y

Rodríguez-Caballero, A., A.C. García-Montero, P. Bárcena, J. Almeida, F. Ruiz-Cabello, M.D. Tabernero, P. Garrido, S. Muñoz-Criado, Y. Sandberg, A.W. Langerak, et al. 2008. Expanded cells in monoclonal TCR-alphabeta+/CD4+/NKa+/CD8-/+dim T-LGL lymphocytosis recognize hCMV antigens. *Blood.* 112:4609–4616. http://dx.doi.org/10.1182/blood-2008-03-146241

Sakata-Yanagimoto, M., T. Enami, K. Yoshida, Y. Shiraishi, R. Ishii, Y. Miyake, H. Muto, N. Tsuyama, A. Sato-Otsubo, Y. Okuno, et al. 2014. Somatic RHOA mutation in angioimmunoblastic T cell lymphoma. *Nat. Genet.* 46:171–175. http://dx.doi.org/10.1038/ng.2872

Salio, M., J.D. Silk, E.Y. Jones, and V. Cerundolo. 2014. Biology of CD1- and MR1-restricted T cells. *Annu. Rev. Immunol.* 32:323–366. http://dx.doi.org/10.1146/annurev-immunol-032713-120243

Shaffer, A.L. III, R.M. Young, and L.M. Staudt. 2012. Pathogenesis of human B cell lymphomas. *Annu. Rev. Immunol.* 30:565–610. http://dx.doi.org/10.1146/annurev-immunol-020711-075027

Shin, H., S.D. Blackburn, J.N. Blattman, and E.J. Wherry. 2007. Viral antigen and extensive division maintain virus-specific CD8 T cells during chronic infection. *J. Exp. Med.* 204:941–949. http://dx.doi.org/10.1084/jem.20061937

Sidobre, S., and M. Kronenberg. 2002. CD1 tetramers: a powerful tool for the analysis of glycolipid-reactive T cells. *J. Immunol. Methods.* 268:107–121. http://dx.doi.org/10.1016/S0022-1759(02)00204-1

Siliceo, M., and I. Mérida. 2009. T cell receptor-dependent tyrosine phosphorylation of beta2-chimaerin modulates its Rac-GAP function in T cells. *J. Biol. Chem.* 284:11354–11363. http://dx.doi.org/10.1074/jbc.M806098200

Streubel, B., U. Vinatzer, M. Willheim, M. Raderer, and A. Chott. 2006. Novel t(5;9)(q33;q22) fuses ITK to SYK in unspecified peripheral T-cell lymphoma. *Leukemia.* 20:313–318. http://dx.doi.org/10.1038/sj.leu.2404045

Suarez, F., O. Lortholary, O. Hermine, and M. Lecuit. 2006. Infection-associated lymphomas derived from marginal zone B cells: a model of antigen-driven lymphoproliferation. *Blood.* 107:3034–3044. http://dx.doi.org/10.1182/blood-2005-09-3679

Subramanian, A., P. Tamayo, V.K. Mootha, S. Mukherjee, B.L. Ebert, M.A. Gillette, A. Paulovich, S.L. Pomeroy, T.R. Golub, E.S. Lander, and J.P. Mesirov. 2005. Gene set enrichment analysis: a knowledge-based approach for interpreting genome-wide expression profiles. *Proc. Natl. Acad. Sci. USA.* 102:15545–15550. http://dx.doi.org/10.1073/pnas.0506580102

Swerdlow, S., E. Campo, and N. Harris. 2008. World Health Organization Classification of Tumors of Haematopoietic and Lymphoid Tissues. IARC Press, Lyon, France. 439 pp.

Travert, M., Y. Huang, L. de Leval, N. Martin-Garcia, M.H. Delfau-Larue, F. Berger, J. Bosq, J. Brière, J. Soulier, E. Macintyre, et al. 2012. Molecular features of hepatosplenic T-cell lymphoma unravels potential novel

therapeutic targets. *Blood*. 119:5795–5806. http://dx.doi.org/10.1182/blood-2011-12-396150

Uldrich, A.P., J. Le Nours, D.G. Pellicci, N.A. Gherardin, K.G. McPherson, R.T. Lim, O. Patel, T. Beddoe, S. Gras, J. Rossjohn, and D.I. Godfrey. 2013. CD1d-lipid antigen recognition by the γδ TCR. *Nat. Immunol.* 14:1137–1145. http://dx.doi.org/10.1038/ni.2713

Vahl, J.C., K. Heger, N. Knies, M.Y. Hein, L. Boon, H. Yagita, B. Polic, and M. Schmidt-Supprian. 2013. NKT cell-TCR expression activates conventional T cells in vivo, but is largely dispensable for mature NKT cell biology. *PLoS Biol.* 11:e1001589. http://dx.doi.org/10.1371/journal.pbio.1001589

Van Rhijn, I., A. Kasmar, A. de Jong, S. Gras, M. Bhati, M.E. Doorenspleet, N. de Vries, D.I. Godfrey, J.D. Altman, W. de Jager, et al. 2013. A conserved human T cell population targets mycobacterial antigens presented by CD1b. *Nat. Immunol.* 14:706–713. http://dx.doi.org/10.1038/ni.2630

Vaqué, J.P., G. Gómez-López, V. Monsálvez, I. Varela, N. Martínez, C. Pérez, O. Domínguez, O. Graña, J.L. Rodríguez-Peralto, S.M. Rodríguez-Pinilla, et al. 2014. PLCG1 mutations in cutaneous T-cell lymphomas. *Blood*. 123:2034–2043. http://dx.doi.org/10.1182/blood-2013-05-504308

Vasmatzis, G., S.H. Johnson, R.A. Knudson, R.P. Ketterling, E. Braggio, R. Fonseca, D.S. Viswanatha, M.E. Law, N.S. Kip, N. Ozsan, et al. 2012. Genome-wide analysis reveals recurrent structural abnormalities of TP63 and other p53-related genes in peripheral T-cell lymphomas. *Blood*. 120:2280–2289. http://dx.doi.org/10.1182/blood-2012-03-419937

Wang, X., M.B. Werneck, B.G. Wilson, H.J. Kim, M.J. Kluk, C.S. Thom, J.W. Wischhusen, J.A. Evans, J.L. Jesneck, P. Nguyen, et al. 2011. TCR-dependent transformation of mature memory phenotype T cells in mice. *J. Clin. Invest.* 121:3834–3845. http://dx.doi.org/10.1172/JCI37210

Wang, Y., I. Misumi, A.D. Gu, T.A. Curtis, L. Su, J.K. Whitmire, and Y.Y. Wan. 2013. GATA-3 controls the maintenance and proliferation of T cells downstream of TCR and cytokine signaling. *Nat. Immunol.* 14:714–722. http://dx.doi.org/10.1038/ni.2623

Ward, J.M., L. Tadesse-Heath, S.N. Perkins, S.K. Chattopadhyay, S.D. Hursting, and H.C. Morse III. 1999. Splenic marginal zone B-cell and thymic T-cell lymphomas in p53-deficient mice. *Lab. Invest.* 79:3–14.

Wherry, E.J. 2011. T cell exhaustion. *Nat. Immunol.* 12:492–499. http://dx.doi.org/10.1038/ni.2035

Wherry, E.J., and R. Ahmed. 2004. Memory CD8 T-cell differentiation during viral infection. *J. Virol.* 78:5535–5545. http://dx.doi.org/10.1128/JVI.78.11.5535-5545.2004

Wieland Brown, L.C., C. Penaranda, P.C. Kashyap, B.B. Williams, J. Clardy, M. Kronenberg, J.L. Sonnenburg, L.E. Comstock, J.A. Bluestone, and M.A. Fischbach. 2013. Production of α-galactosylceramide by a prominent member of the human gut microbiota. *PLoS Biol.* 11:e1001610. http://dx.doi.org/10.1371/journal.pbio.1001610

Wilson, M.T., C. Johansson, D. Olivares-Villagómez, A.K. Singh, A.K. Stanic, C.R. Wang, S. Joyce, M.J. Wick, and L. Van Kaer. 2003. The response of natural killer T cells to glycolipid antigens is characterized by surface receptor down-modulation and expansion. *Proc. Natl. Acad. Sci. USA*. 100:10913–10918. http://dx.doi.org/10.1073/pnas.1833166100

Wingender, G., P. Rogers, G. Batzer, M.S. Lee, D. Bai, B. Pei, A. Khurana, M. Kronenberg, and A.A. Horner. 2011. Invariant NKT cells are required for airway inflammation induced by environmental antigens. *J. Exp. Med.* 208:1151–1162. http://dx.doi.org/10.1084/jem.20102229

Yoo, H.Y., M.K. Sung, S.H. Lee, S. Kim, H. Lee, S. Park, S.C. Kim, B. Lee, K. Rho, J.E. Lee, et al. 2014. A recurrent inactivating mutation in RHOA GTPase in angioimmunoblastic T cell lymphoma. *Nat. Genet.* 46:371–375. http://dx.doi.org/10.1038/ng.2916

Yu, J., T. Mitsui, M. Wei, H. Mao, J.P. Butchar, M.V. Shah, J. Zhang, A. Mishra, C. Alvarez-Breckenridge, X. Liu, et al. 2011. NKp46 identifies an NKT cell subset susceptible to leukemic transformation in mouse and human. *J. Clin. Invest.* 121:1456–1470. http://dx.doi.org/10.1172/JCI43242